42. Yokoyama, Y., Kuramitsu, Y., Takashima, M., Iizuka, N., Toda, T., Terai, S., Sakaida, I., Oka, M., Nakamura, K., and Okita, K. (2004) Proteomic profiling of proteins decreased in hepatocellular carcinoma from patients infected with hepatitis C virus. *Proteomics* **4**, 2111–2116
43. Moradpour, D., Englert, C., Wakita, T., and Wands, J.R. (1996) Characterization of cell lines allowing tightly regulated expression of hepatitis C virus core protein. *Virology* **222**, 51–63
44. Hope, R.G. and McLauchlan, J. (2000) Sequence motifs required for lipid droplet association and protein stability are unique to the hepatitis C virus core protein. *J. Gen. Virol.* **81**, 1913–1925
45. Hope, R.G., Murphy, D.J., and McLauchlan, J. (2002) The domains required to direct core proteins of hepatitis C virus and GB virus-B to lipid droplets share common features with plant oleosin proteins. *J. Biol. Chem.* **277**, 4261–4270
46. Shi, S.T., Polyak, S.J., Tu, H., Taylor, D.R., Gretch, D.R., and Lai, M.M. (2002) Hepatitis C virus NS5A colocalizes with the core protein on lipid droplets and interacts with apolipoproteins. *Virology* **292**, 198–210
47. Harada, T., Kim, D.W., Sagawa, K., Suzuki, T., Takahashi, K., Saito, I., Matsuura, Y., and Miyamura, T. (1995) Characterization of an established human hepatoma cell line constitutively expressing non-structural proteins of hepatitis C virus by transfection of viral cDNA. *J. Gen. Virol.* **76**, 1215–1221
48. Balch, W.E. and Rothman, J.E. (1985) Characterization of protein transport between successive compartments of the Golgi apparatus: asymmetric properties of donor and acceptor activities in a cell-free system. *Arch. Biochem. Biophys.* **240**, 413–425
49. Yanagida, M., Miura, Y., Yagasaki, K., Taoka, M., Isobe, T., and Takahashi, N. (2000) Matrix assisted laser desorption/ionization-time of flight-mass spectrometry analysis of proteins detected by anti-phosphotyrosine antibody on two-dimensional-gels of fibrolast cell lysates after tumor necrosis factor-alpha stimulation. *Electrophoresis* **21**, 1890–1898
50. Yanagida, M., Shimamoto, A., Nishikawa, K., Furuichi, Y., Isobe, T., and Takahashi, N. (2001) Isolation and proteomic characterization of the major proteins of the nucleolin-binding ribonucleoprotein complexes. *Proteomics* **1**, 1390–1404
51. Bligh, E.G. and Dyer, W.J. (1959) A rapid method of total lipid extraction and purification. *Can. J. Med. Sci.* **37**, 911–917
52. Natsume, T., Yamauchi, Y., Nakayama, H., Shinkawa, T., Yanagida, M., Takahashi, N., and Isobe, T. (2002) A direct nanoflow liquid chromatography-tandem mass spectrometry system for interaction proteomics. *Anal. Chem.* **74**, 4725–4733
53. Yanagida, M., Hayano, T., Yamauchi, Y., Shinkawa, T., Natsume, T., Isobe, T., and Takahashi, N. (2004) Human fibrillarin forms a sub-complex with splicing factor 2-associated p32, protein arginine methyltransferases, and tubulins alpha 3 and beta 1 that is independent of its association with preribosomal ribonucleoprotein complexes. *J. Biol. Chem.* **279**, 1607–1614
54. Heid, H.W., Moll, R., Schwetlick, I., Rackwitz, H.R., and Keenan, T.W. (1998) Adipophilin is a specific marker of lipid accumulation in diverse cell types and diseases. *Cell Tissue Res.* **294**, 309–321
55. Londos, C., Brasaemle, D.L., Schultz, C.J., Segrest, J.P., and Kimmel, A.R. (1999) Perilipins, ADRP, and other proteins that associate with intracellular neutral lipid droplets in animal cells. *Semin. Cell Dev. Biol.* **10**, 51–58
56. Wolins, N.E., Rubin, B. and Brasaemle, D.L. (2001) TIP47 associates with lipid droplets. *J. Biol. Chem.* **276**, 5101–5108
57. Miura, S., Gan, J.W., Brzostowski, J., Parisi, M.J., Schultz, C.J., Londos, C., Oliver, B., and Kimmel, A.R. (2002) Functional conservation for lipid storage droplet association among Perilipin, ADRP, and TIP47 (PAT)-related proteins in mammals, Drosophila, and Dictyostelium. *J. Biol. Chem.* **277**, 32253–32257
58. Liu, P., Ying, Y., Zhao, Y., Mundy, D.I., Zhu, M., and Anderson, R.G. (2004) Chinese hamster ovary K2 cell lipid droplets appear to be metabolic organelles involved in membrane traffic. *J. Biol. Chem.* **279**, 3787–3792
59. Fujimoto, Y., Itabe, H., Sakai, J., Makita, M., Noda, J., Mori, M., Higashi, Y., Kojima, S., and Takano, T. (2004) Identification of major proteins in the lipid droplet-enriched fraction isolated from the human hepatocyte cell line HuH7. *Biochim. Biophys. Acta* **1644**, 47–59
60. Brasaemle, D.L., Dolios, G., Shapiro, L., and Wang, R. (2004) Proteomic analysis of proteins associated with lipid droplets of basal and lipolytically stimulated 3T3-L1 adipocytes. *J. Biol. Chem.* **279**, 46835–46842
61. Lu, X., Gruia-Gray, J., Copeland, N.G., Gilbert, D.J., Jenkins, N.A., Londos, C., and Kimmel, A.R. (2001) The murine perilipin gene: the lipid droplet-associated perilipins derive from tissue-specific, mRNA splice variants and define a gene family of ancient origin. *Mamm. Genome* **12**, 741–749
62. Greenberg, A.S., Egan, J.J., Wek, S.A., Moos, M.C., Jr., Londos, C., and Kimmel, A.R. (1993) Isolation of cDNAs for perilipins A and B: sequence and expression of lipid droplet-associated proteins of adipocytes. *Proc. Natl. Acad. Sci. USA* **90**, 12035–12039
63. Diaz, E. and Pfeffer, S.R. (1998) TIP47: a cargo selection device for mannose 6-phosphate receptor trafficking. *Cell* **93**, 433–443
64. Brasaemle, D.L., Barber, T., Wolins, N.E., Serrero, G., Blanchette-Mackie, E.J., and Londos, C. (1997) Adipose differentiation-related protein is an ubiquitously expressed lipid storage droplet-associated protein. *J. Lipid Res.* **38**, 2249–2263
65. Carroll, K.S., Hanna, J., Simon, I., Krise, J., Barbero, P., and Pfeffer, S.R. (2001) Role of Rab9 GTPase in facilitating receptor recruitment by TIP47. *Science* **292**, 1373–1376
66. Pfeffer, S.R. (2001) Rab GTPases: specifying and deciphering organelle identity and function. *Trends Cell Biol.* **11**, 487–491
67. Blot, G., Janvier, K., Le Panse, S., Benarous, R., and Berlioz-Torrent, C. (2003) Targeting of the human immunodeficiency virus type 1 envelope to the trans-Golgi network through binding to TIP47 is required for env incorporation into virions and infectivity. *J. Virol.* **77**, 6931–6945
68. Serfaty, L., Andreani, T., Giral, P., Carbonell, N., Chazouilleres, O., and Poupon, R. (2001) Hepatitis C virus induced hypobetalipoproteinemia: a possible mechanism for steatosis in chronic hepatitis C. *J. Hepatol.* **34**, 428–434
69. Perlemuter, G., Sabile, A., Letteron, P., Vona, G., Topilco, A., Chretien, Y., Koike, K., Pessayre, D., Chapman, J., Barba, G., and Brechot, C. (2002) Hepatitis C virus core protein inhibits microsomal triglyceride transfer protein activity and very low density lipoprotein secretion: a model of viral-related steatosis. *FASEB J.* **16**, 185–194
70. Owsianka, A.M. and Patel, A.H. (1999) Hepatitis C virus core protein interacts with a human DEAD box protein DDX3. *Virology* **257**, 330–340
71. Mamiya, N. and Worman, H.J. (1999) Hepatitis C virus core protein binds to a DEAD box RNA helicase. *J. Biol. Chem.* **274**, 15751–15756
72. Gururajan, R. and Weeks, D.L. (1997) An3 protein encoded by a localized maternal mRNA in Xenopus laevis is an ATPase with substrate-specific RNA helicase activity. *Biochim. Biophys. Acta* **1350**, 169–182
73. Chen, H.C., Lin, W.C., Tsay, Y.G., Lee, S.C., and Chang, C.J. (2002) An RNA helicase, DDX1, interacting with poly(A) RNA and heterogeneous nuclear ribonucleoprotein K. *J. Biol. Chem.* **277**, 40403–40409
74. Dvorak, A.M., Morgan, E.S., and Weller, P.F. (2003) RNA is closely associated with human mast cell lipid bodies. *Histol. Histopathol.* **18**, 943–968
75. Godbout, R., Packer, M., and Bie, W. (1998) Overexpression of a DEAD box protein (DDX1) in neuroblastoma and retinoblastoma cell lines. *J. Biol. Chem.* **273**, 21161–21168

76. Huang, J.S., Chao, C.C., Su, T.L., Yeh, S.H., Chen, D.S., Chen, C.T., Chen, P.J., and Jou, Y.S. (2004) Diverse cellular transformation capability of overexpressed genes in human hepatocellular carcinoma. *Biochem. Biophys. Res. Commun.* **315**, 950–958
77. Liu, M., Liu, Y., Cheng, J., Zhang, S.L., Wang, L., Shao, Q., Zhang, J., and Yang, Q. (2004) Transactivating effect of hepatitis C virus core protein: a suppression subtractive hybridization study. *World J. Gastroenterol.* **10**, 1746–1749
78. Ohkawa, K., Ishida, H., Nakanishi, F., Hosui, A., Sato, A., Ueda, K., Takehara, T., Kasahara, A., Sasaki, Y., Hori, M., and Hayashi, N. (2003) Changes in gene expression profile by HCV core protein in cultured liver cells: analysis by DNA array assay. *Hepatol. Res.* **25**, 396–408
79. Sacco, R., Tsutsumi, T., Suzuki, R., Otsuka, M., Aizaki, H., Sakamoto, S., Matsuda, M., Seki, N., Matsuura, Y., Miyamura, T., and Suzuki, T. (2003) Antiapoptotic regulation by hepatitis C virus core protein through up-regulation of inhibitor of caspase-activated DNase. *Virology* **317**, 24–35

Enhancement of *de Novo* Fatty Acid Biosynthesis in Hepatic Cell Line Huh7 Expressing Hepatitis C Virus Core Protein

Masayoshi FUKASAWA,*[,a] Yasuhito TANAKA,[a] Shigeko SATO,[a] Yujin ONO,[a] Yuko NITAHARA-KASAHARA,[a] Tetsuro SUZUKI,[b] Tatsuo MIYAMURA,[b] Kentaro HANADA,[a] and Masahiro NISHIJIMA[a,c]

[a] *Department of Biochemistry and Cell Biology, National Institute of Infectious Diseases; and* [b] *Department of Virology II, National Institute of Infectious Diseases; Tokyo 162–8640, Japan: and* [c] *Department of Clinical Pharmacy, Faculty of Pharmaceutical Sciences, Doshisha Women's College of Liberal Arts; Kyoto 610–0395, Japan.*
Received June 12, 2006; accepted July 7, 2006; published online July 10, 2006

Hepatitis C virus (HCV) core protein plays important roles in the pathogeneses of liver steatosis as well as hepatocellular carcinomas due to HCV infection. In this study, we examined *de novo* fatty acid biosynthesis in hepatic cell line Huh7 cells expressing HCV core protein. The rate of metabolic labeling of cellular fatty acids with [^{3}H]acetate in core-expressing (Uc39-6) cells was *ca.* 1.5-fold higher than that in non-expressing (Uc321) cells. The enzyme activities responsible for fatty acid biosynthesis were assayed *in vitro*. Cytosolic acetyl-CoA carboxylase activity in Uc39-6 cells was *ca.* 1.6-fold higher than that in Uc321 cells. On the other hand, cytosolic fatty acid synthase activity in Uc39-6 cells was only slightly higher than that in Uc321 cells. Immunoblot analysis of acetyl-CoA carboxylase 1 (ACC1), which is a rate-limiting enzyme for fatty acid biosynthesis, revealed a higher expression level of the protein in Uc39-6 cells than in Uc321 cells. The ACC1 mRNA content in Uc39-6 cells was 1.4-fold higher than that in Uc321 cells. These results strongly suggest that enhancement of fatty acid biosynthesis in core-expressing cells is caused by increased expression of fatty acid biosynthetic enzymes, especially ACC1. Up-regulation of *de novo* fatty acid biosynthesis by HCV core protein may affect cellular lipid metabolism, resulting in neutral lipid accumulation in HCV-infected cells.

Key words fatty acid biosynthesis; hepatitis C virus; acetyl-CoA carboxylase; fatty acid synthase

Hepatitis C virus (HCV) is a major causative agent of chronic hepatitis.[1,2] Persistent HCV infection, which develops in at least 70 to 80% of infected patients, is strongly correlated with the development of severe liver diseases such as cirrhosis and hepatocellular carcinomas (HCC).[3,4] In addition, liver steatosis, which involves the accumulation of intracellular neutral lipids as lipid droplets, is a hallmark of chronic HCV infection,[5] and is suggested to play a central role in the progression of the following liver cirrhosis and HCC in chronic hepatitis C patients.[6] Since more than 170 million people in the world are currently infected with HCV,[1] understanding the mechanisms by which HCV induces serious liver diseases is one of the most important global public health issues.

HCV, belonging to the *Flaviviridae* family, possesses a linear, positive-stranded RNA genome of *ca.* 9600 nucleotides.[7] The HCV genome has a single open reading frame encoding a precursor polyprotein of *ca.* 3000 amino acids that is processed into at least 10 individual proteins by host and viral proteases.[8] HCV core protein, the product of the N-terminal portion of the polyprotein, forms the nucleocapsid of an HCV virion.[9] Besides its function as a viral structural protein, the core protein causes intracellular lipid accumulation as well as malignant transformation in cultured cells.[10—13] Moreover, transgenic mice expressing HCV core protein developed liver steatosis and the following HCC.[14,15] These results strongly suggest that HCV core protein is involved in the pathogeneses of liver diseases including steatosis due to HCV infection.

The details of the mechanisms by which HCV core protein causes intracellular neutral lipid accumulation are not well understood. Extensive screening for genes/proteins exhibiting differences in cellular expression involving cDNA microarray or proteome analysis has been performed for HCV core-expressing cultured liver cells or transgenic mice.[16—19] Although various genes/proteins were identified, direct information on the genes/proteins related to lipid metabolism altered by HCV core protein expression has not been obtained yet. Since HCV core protein is distributed mainly in lipid droplets of host cells,[10,13,20—23] the biogenesis and/or functions of lipid droplets might be affected by the core protein. As reported, the core protein appears to inhibit microsomal triglyceride transfer protein activity in the livers of HCV core-transgenic mice, thus interfering with the hepatic assembly and secretion of apo-B-carrying very low density lipoproteins.[24] As a result, triglycerides appear to accumulate within hepatocytes, steatosis developing. HCV core protein also interacts with apoA2, a major component of high-density lipoproteins, in cells.[10,25] These results should be important regarding the pathogenesis of HCV core-derived steatosis, but may not explain all the functions of the core protein causing intracellular neutral lipid accumulation. In this study, we investigated *de novo* fatty acid biosynthesis, which can significantly affect intracellular lipid metabolism, especially neutral lipid accumulation,[26,27] in HCV core-expressing liver cells. We found elevated fatty acid biosynthesis, and higher expression and activities of the enzymes responsible for *de novo* fatty acid biosynthesis in HCV core-expressing cells.

MATERIALS AND METHODS

Cell Lines The human hepatic Huh7 cell line constitutively expressing HCV core protein (Uc39-6) was established by transfection with pcEF39neo.[28] Expression level of HCV core protein in Uc39-6 cells was similar to that in core-expressing Hep39 cells (data not shown), which we established previously.[28,29] Another Huh7 cell line transfected with ex-

* To whom correspondence should be addressed. e-mail: fuka@nih.go.jp

pression vector pcEF321swxneo[28] without the HCV core protein insert (Uc321) was used as a mock control. Both cell lines were plated on collagen-coated dishes (Asahi Techno Glass, Japan) and maintained in normal culture medium (DMEM supplemented with 10% fetal bovine serum, 100 units/ml penicillin G, 100 μg/ml streptomycin sulfate, and 1 mg/ml G418 (Sigma, U.S.A.)) under a 5% CO_2 atmosphere at 37°C. Growth rates under the culture condition we used were comparable between Uc321 and Uc39-6 cells.

Metabolic Labeling of Cellular Lipids Subconfluent cell monolayers in 6-cm dishes were incubated in 2 ml of the normal medium containing 1.3 μM [^{3}H]acetate (Moravek Biochemicals, U.S.A.) for various times. After being washed three times with 3 ml of PBS, the cells were lysed in 1 ml of 0.1% SDS at 4°C, and then 100 and 800 μl aliquots of the resultant cell lysate were used for protein determination and lipid extraction, respectively. Cellular lipids were extracted into the organic solvent[30] and dried up. To determine the total metabolic incorporation of [^{3}H]acetate into the fatty acid moieties of lipids, the extracted lipids were treated with 90% ethanol containing 1 N KOH for 1 h at 70°C and then re-extracted with petroleum ether. Fatty acids were then separated on TLC plates with a solvent system of hexane/diethylether/acetate (70/30/1, vol/vol). The radioactivity of fatty acids was determined with a BAS1800 imaging analysis system (Fuji Film, Japan). The values were normalized as to cell protein.

***In Vitro* Acetyl-CoA Carboxylase (ACC) and Fatty Acid Synthase (FAS) Activity Assays** ACC activity assays were performed using [^{14}C] $KHCO_3$ (American Radiolabeled Chemicals, U.S.A.).[31] FAS activity was measured using [^{14}C]acetyl-CoA (Moravek Biochemicals, U.S.A.).[32] Cytosolic fractions, which contain ACC1 and FAS, were prepared as below. After being washed with PBS, cells were harvested and precipitated by centrifugation (300×g, 5 min). The precipitated cells were resuspended in 125 mM potassium phosphate, pH 7.0, and then lysed by sonication. After centrifugation of each lysate at 2500×g for 5 min, the cytosolic fraction (supernatant) was separated from the post-nuclear supernatant by centrifugation at 100000×g for 60 min. The protein concentrations of the preparations were determined with a BCA protein assay kit (Pierce, U.S.A.).

Immunoblot Analysis Equivalent amounts of proteins from Uc321 and Uc39-6 cells were separated in a 4—12% SDS-polyacrylamide gel and then electrophoretically transferred to polyvinylidene difluoride membranes. The membranes were blocked overnight at 4°C in TBS containing 0.1% Tween 20 and 5% skim milk. The blots were probed with a rabbit polyclonal anti-ACC1 antibody (Upstate, U.S.A.) (1 : 1000), a mouse monoclonal anti-FAS antibody (BD Transduction Laboratories, U.S.A.) (1 : 1000), and a mouse monoclonal anti-HCV core protein antibody (Anogen, Canada) (1 : 2000) for 90 min at room temperature. The blots were then incubated with horseradish peroxidase-conjugated goat anti-rabbit IgG (BIO-RAD, U.S.A.), or HRP-conjugated goat anti-mouse IgG (GE Healthcare, U.S.A.) at 1 : 2000 dilution for 60 min. Detection of immunoreactive proteins was performed with an ECL system (GE Healthcare, U.S.A.).

Quantitative Real-Time PCR Analysis Cellular total RNAs were prepared with an RNeasy kit (Qiagen, U.S.A.). The total RNA fraction (1 μg) was processed directly to cDNA using a Transcriptor First Strand cDNA Synthesis Kit (Roche, U.S.A.). Of the total 20 μl cDNA solution, an aliquot of 0.5 μl was used for each real-time PCR assay. The PCR primers used for human ACC1 were: forward, CTGTTGGCTCAGATACACTC, and reverse, GCCACAGTGAAATCTCGTT. The PCR primers for human FAS were: forward, GTGGGAAGGTGTACCAGTG, and reverse, AGGATGCCCTGGAAATGAG. Quantitative real-time PCR was carried out in a LightCycler (Roche, U.S.A.) using LightCycler-FastStart DNA Master SYBR Green I (Roche, U.S.A.). Specific PCR products amplified against individual genes were used as quantitative standards.

RESULTS

To determine the effect of HCV core protein expression on cellular fatty acid biosynthesis, we established Uc39-6 cells, a human hepatic Huh7 cell line transfected with the pcEF321 mammalian expression vector containing the HCV core protein gene, and Uc321 cells, a control Huh7 cell line transfected with the pcEF321 vector without the core protein gene. Consistent with previous studies involving HCV core-expressing hepatic cell lines,[10,33] HCV core protein was preferentially distributed in the endoplasmic reticulum and lipid droplets in Uc39-6 cells, as determined on immunofluorescence microscopy (data not shown). *De novo* fatty acid biosynthesis in HCV core-expressing and non-expressing cells was examined by metabolic labeling with [^{3}H]acetate. Most biosynthesized [^{3}H]fatty acids were rapidly incorporated into complex lipids such as phospholipids, triglycerides, and cholesteryl esters, but free [^{3}H]fatty acids were not detectable (<1/1000 of total [^{3}H]fatty acids formed) in these cells. Incorporation of radioactivity into the fatty acid moieties of complex lipids was *ca.* 1.5-fold higher in HCV core-expressing Uc39-6 cells than that in non-expressing Uc321 cells during the incubation time at 37°C (Fig. 1). Similar results were obtained with other Huh7 cell lines expressing HCV core protein (data not shown), ruling out the possibility that the increase in radiolabeled fatty acids in HCV core-expressing cells are due to the peculiar cell clones. These results indicate that the rate of *de novo* biosynthesis of cellular fatty acids is enhanced in HCV core-expressing cells.

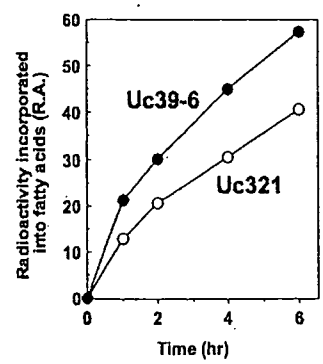

Fig. 1. Fatty Acid Biosynthesis in HCV Core-Expressing Uc39-6 and Control Uc321 Cells

Cells were metabolically labeled with [^{3}H]acetate for the indicated times. The radioactivity incorporated into the fatty acid moieties of lipids was determined as described under Materials and Methods. Open circles, Uc321 cells; closed circles, Uc39-6 cells. R.A., relative radioactivity. Data are representative of four independent experiments.

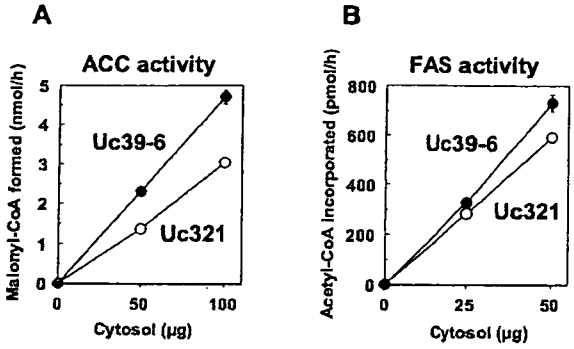

Fig. 2. ACC and FAS Activities in Uc321 and Uc39-6 Cytosolic Fractions

In vitro activity assaying of ACC (A) and FAS (B) was performed as described under Materials and Methods. Open circles, Uc321 cells; closed circles, Uc39-6 cells. Data are expressed as means±S.D. for three determinations.

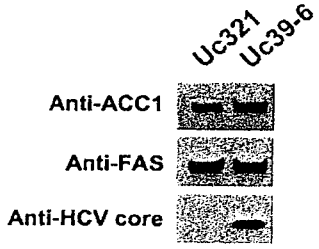

Fig. 3. Immunoblot Analysis of ACC1 and FAS in Uc321 and Uc39-6 Cells

Total cell lysates (30 μg of protein per lane) of Uc321 and Uc39-6 cells were analyzed by immunoblotting with anti-ACC1, anti-FAS, and anti-HCV core antibodies.

Fatty acid biosynthesis is carried out by cytosolic enzymes, *i.e.*, ACC1 and FAS.[34] We assayed these enzyme activities in cytosolic fractions of Uc321 and Uc39-6 cells. HCV core-expressing Uc39-6 cells showed a *ca.*1.6-fold higher level of ACC activity than Uc321 cells (Fig. 2A). The cytosolic FAS activity in Uc39-6 cells was slightly higher than that in Uc321 cells (Fig. 2B). These results demonstrate that the enzymatic activities responsible for fatty acid biosynthesis, especially ACC activity, are elevated in HCV core-expressing Uc39-6 cells, consistent with the results of metabolic labeling experiments involving [^{3}H]acetate.

Cytosolic ACC and FAS activities are attributed to ACC1 and FAS molecules, respectively.[34] We next performed immunoblot analyses of ACC1 and FAS molecules in lysates of Uc321 and Uc39-6 cells. Uc39-6 cells contained a *ca.* 2-fold higher amount of ACC1 protein than Uc321 cells (Fig. 3), whereas the protein level of FAS in UC39-6 cells was comparable to that in Uc321 cells. These results suggest that the elevated protein level of ACC1, a rate-limiting enzyme for fatty acid biosynthesis, may contribute to the higher ACC activity, leading to enhanced fatty acid biosynthesis, in HCV core-expressing Uc39-6 cells. We also determined the mRNA levels of ACC1 and FAS in Uc321 and Uc39-6 cells by quantitative real-time PCR. Consistent with the protein levels of ACC1, the ACC1 mRNA content in Uc39-6 cells was significantly higher than that in Uc321 cells (Fig. 4A). The FAS mRNA content in Uc39-6 cells was also higher than that in Uc321 cells (Fig. 4B). These results suggest that elevated expression of the ACC1 (and FAS) gene(s) causes a higher rate of *de novo* fatty acid biosynthesis in HCV core-expressing cells.

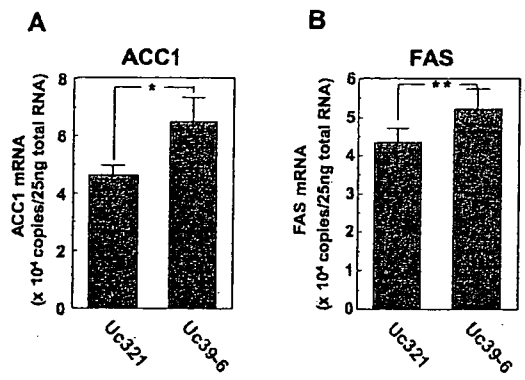

Fig. 4. ACC1 and FAS mRNA Levels in Uc321 and Uc39-6 Cells

Total RNA was isolated from Uc321 and Uc39-6 cells, and the ACC1 (A) and FAS (B) mRNA levels were determined by quantitative real-time PCR. Data are expressed as means±S.D. for three determinations. Statistical significance of differences in mRNA levels between Uc321 and Uc39-6 cells was evaluated using Student's *t* test. $*p<0.01$, $**p<0.025$.

DISCUSSION

In this study we showed that the rate of *de novo* fatty acid biosynthesis was elevated in HCV core-expressing cells (Fig. 1). We also demonstrated that the protein and mRNA expression levels as well as the *in vitro* enzymatic activity of ACC1, which is a rate-limiting key enzyme for fatty acid biosynthesis, were significantly enhanced in HCV core-expressing Uc39-6 cells (Figs. 2—4). These results strongly suggest that the higher expression of ACC1 contributes to the increased fatty acid biosynthesis in HCV core-expressing cells.

Many studies have demonstrated that HCV core protein substantially affects various cellular regulatory processes including gene transcription.[35—37] These biological activities of HCV core protein might be involved in the mechanism by which HCV core protein enhances expression of the ACC1 gene.

HCV core protein is localized mainly in lipid droplets of host cells,[10,13,20—23] and a small portion of ACC1 molecules is also associated with lipid droplets.[38] It is well known that the activity of ACC1 can be regulated posttranslationally through its phosphorylation, and allosteric effectors such as citrate and fatty acids.[39] Thus, we can not exclude the possibility that HCV core protein activates ACC1 directly in lipid droplets, although we have not examined this yet.

We also found that the FAS mRNA expression level was slightly enhanced, but the protein level as well as the *in vitro* enzymatic activity of FAS were not significantly elevated in Uc39-6 cells (Figs. 2—4). FAS appears to make a lesser contribution to the enhancement of fatty acid biosynthesis in Uc39-6 cells under our culture conditions, although further investigations are needed.

We think that our findings may provide a new insight into the metabolic pathways for lipids by which HCV core protein causes steatosis, one of the characteristic indications of chronic hepatitis C infection. Although in the future we have to determine whether or not our *in vitro* findings are applicable to an *in vivo* situation on HCV infection, inhibition of ACC1 and/or FAS activity might be effective for preventing the liver steatosis due to HCV infection.

Acknowledgements This work was supported by

Grants-in-Aid from the Ministry of Health, Labor and Welfare; the program for the Promotion of Fundamental Studies in Health Sciences of the Organization for Drug ADR Relief, R&D Promotion, and Product Review of Japan; the Takeda Science Foundation; and the Viral Hepatitis Research Foundation of Japan.

REFERENCES AND NOTES

1) Choo Q. L., Kuo G., Weiner A. J., Overby L. R., Bradley D. W., Houghton M., *Science*, **244**, 359—362 (1989).
2) Kuo G., Choo Q. L., Alter H. J., Gitnick G. L., Redeker A. G., Purcell R. H., Miyamura T., Dienstag J. L., Alter M. J., Stevens C. E., Tegtmeier G. E., Bonino F., Colombo M., Lee W.-S., Kuo C., Berger K., Shuster J. R., Overby L. R., Bradley D. W., Houghton M., *Science*, **244**, 362—364 (1989).
3) Saito I., Miyamura T., Ohbayashi A., Harada H., Katayama T., Kikuchi S., Watanabe Y., Koi S., Onji M., Ohta Y., Choo Q.-L., Houghton M., Kuo G., *Proc. Natl. Acad. Sci. U.S.A.*, **87**, 6547—6549 (1990).
4) Kiyosawa K., Sodeyama T., Tanaka E., Gibo Y., Yoshizawa K., Nakano Y., Furuta S., Akahane Y., Nishioka K., Purcell R. H., Alter H. J., *Hepatology*, **12**, 671—675 (1990).
5) Goodman Z. D., Ishak K. G., *Semin. Liver Dis.*, **15**, 70—81 (1995).
6) Adinolfi L. E., Durante-Mangoni E., Zampino R., Ruggiero G., *Aliment. Pharmacol. Ther.*, **22** (Suppl. 2), 52—55 (2005).
7) Bartenschlager R., Lohmann V., *J. Gen. Virol.*, **81**, 1631—1648 (2000).
8) Grakoui A., Wychowski C., Lin C., Feinstone S. M., Rice C. M., *J. Virol.*, **67**, 1385—1395 (1993).
9) Santolini E., Migliaccio G., La Monica N., *J. Virol.*, **68**, 3631—3641 (1994).
10) Barba G., Harper F., Harada T., Kohara M., Goulinet S., Matsuura Y., Eder G., Schaff Z., Chapman M. J., Miyamura T., Brechot C., *Proc. Natl. Acad. Sci. U.S.A.*, **94**, 1200—1205 (1997).
11) Ray R. B., Lagging L. M., Meyer K., Ray R., *J. Virol.*, **70**, 4438—4443 (1996).
12) Yoshida T., Hanada T., Tokuhisa T., Kosai K., Sata M., Kohara M., Yoshimura A., *J. Exp. Med.*, **196**, 641—653 (2002).
13) Moradpour D., Englert C., Wakita T., Wands J. R., *Virology*, **222**, 51—63 (1996).
14) Moriya K., Yotsuyanagi H., Shintani Y., Fujie H., Ishibashi K., Matsuura Y., Miyamura T., Koike K., *J. Gen. Virol.*, **78**, 1527—1531 (1997).
15) Moriya K., Fujie H., Shintani Y., Yotsuyanagi H., Tsutsumi T., Ishibashi K., Matsuura Y., Kimura S., Miyamura T., Koike K., *Nat. Med.*, **4**, 1065—1067 (1998).
16) Sacco R., Tsutsumi T., Suzuki R., Otsuka M., Aizaki H., Sakamoto S., Matsuda M., Seki N., Matsuura Y., Miyamura T., Suzuki T., *Virology*, **317**, 24—35 (2003).
17) Li K., Prow T., Lemon S. M., Beard M. R., *Hepatology*, **35**, 1237—1246 (2002).
18) Liu M., Zhang S. L., Cheng J., Liu Y., Wang L., Shao Q., Zhang J., Lin S. M., *World J. Gastroenterol.*, **11**, 3351—3356 (2005).
19) Yamaguchi A., Tazuma S., Nishioka T., Ohishi W., Hyogo H., Nomura S., Chayama K., *Dig. Dis. Sci.*, **50**, 1361—1371 (2005).
20) Hope R. G., McLauchlan J., *J. Gen. Virol.*, **81**, 1913—1925 (2000).
21) Hope R. G., Murphy D. J., McLauchlan J., *J. Biol. Chem.*, **277**, 4261—4270 (2002).
22) Shi S. T., Polyak S. J., Tu, H., Taylor D. R., Gretch D. R., Lai, M. M., *Virology*, **292**, 198—210 (2002).
23) McLauchlan J., Lemberg M. K., Hope G., Martoglio B., *EMBO J.*, **21**, 3980—3988 (2002).
24) Perlemuter G., Sabile A., Letteron P., Vona G., Topilco A., Chretien Y., Koike K., Pessayre D., Chapman J., Barba G., Brechot C., *FASEB J.*, **16**, 185—194 (2002).
25) Sabile A., Perlemuter G., Bono F., Kohara K., Demaugre F., Kohara M., Matsuura Y., Miyamura T., Brechot C., Barba G., *Hepatology*, **30**, 1064—1076 (1999).
26) Girard J., Perdereau D., Foufelle F., Prip-Buus C., Ferre P., *FASEB J.*, **8**, 36—42 (1994).
27) Korczynska J., Stelmanska E., Nogalska A., Szolkiewicz M., Goyke E., Swierczynski J., Rutkowski B., *Metabolism*, **53**, 1060—1065 (2004).
28) Harada T., Kim D. W., Sagawa K., Suzuki T., Takahashi K., Saito I., Matsuura Y., Miyamura T., *J. Gen. Virol.*, **76**, 1215—1221 (1995).
29) Sato S., Fukasawa M., Yamakawa Y., Natsume T., Suzuki T., Shoji I., Aizaki H., Miyamura T., Nishijima M., *J. Biochem.* (Toyko), **139**, 921—930 (2006).
30) Bligh E. G., Dyer W. J., *Can. J. Biochem. Physiol.*, **37**, 911—917 (1959).
31) Nakanishi S., Numa S., *Eur. J. Biochem.*, **16**, 161—173 (1970).
32) Hsu R. Y., Wasson G., Porter J. W., *J. Biol. Chem.*, **240**, 3736—3746 (1965).
33) Ruggieri A., Harada T., Matsuura Y., Miyamura T., *Virology*, **229**, 68—76 (1997).
34) Shi Y., Burn P., *Nat. Rev. Drug Discov.*, **3**, 695—710 (2004).
35) Kim D. W., Suzuki R., Harada T., Saito I., Miyamura T., *Jpn. J. Med. Sci. Biol.*, **47**, 211—220 (1994).
36) Ray R. B., Steele R., Meyer K., Ray R., *J. Biol. Chem.*, **272**, 10983—10986 (1997).
37) Shrivastava A., Manna S. K., Ray R., Aggarwal B. B., *J. Virol.*, **72**, 9722—9728 (1998).
38) Liu P., Ying Y., Zhao Y., Mundy D. I., Zhu M., Anderson R. G., *J. Biol. Chem.*, **279**, 3787—3792 (2004).
39) Kim K. H., *Annu. Rev. Nutr.*, **17**, 77—99 (1997).

Available online at www.sciencedirect.com
SCIENCE DIRECT®
Biochemical and Biophysical Research Communications 336 (2005) 572–578
BBRC
www.elsevier.com/locate/ybbrc

Reduction of hepatitis C virus NS5A phosphorylation through its interaction with amphiphysin II ☆

Atsuko Masumi [a,*], Hideki Aizaki [b], Tetsuro Suzuki [b], James B. DuHadaway [d], George C. Prendergast [d], Katsutoshi Komuro [a], Hidesuke Fukazawa [c]

[a] *Department of Safety Research on Blood and Biological Products, National Institute of Infectious Diseases, Tokyo, Japan*
[b] *Department of Virology II, National Institute of Infectious Diseases, Tokyo, Japan*
[c] *Department of Bioactive Molecules, National Institute of Infectious Diseases, Tokyo, Japan*
[d] *Lankenau Institute for Medical Research, Wynnewood, PA 19096, USA*

Received 8 August 2005
Available online 26 August 2005

Abstract

Hepatitis C virus non-structural protein 5A (NS5A) is a pleiotropic protein with key roles in viral RNA replication, modulation of cellular-signaling pathways and interferon (IFN) responses. To search for possible host factors involved in mediating these functions of NS5A, we adopted an affinity purification approach coupled with mass spectrometry to examine protein–protein interactions, and found that human amphiphysin II (also referred to as Bin1) specifically interacts with NS5A in mammalian cells. Pull-down assays showed that the Src homology 3 (SH3) domain of amphiphysin II is required for NS5A interaction and that c-Src also interacts with NS5A in cells. IFN-α treatment reduced the interaction of NS5A with c-Src, but not amphiphysin II, suggesting that the latter is independent of the IFN-signaling pathway. NS5A is a phosphoprotein and its phosphorylation status is considered to have an effect on viral RNA replication. In vitro kinase assays demonstrated that its interaction with amphiphysin II inhibits phosphorylation of NS5A. These results suggest that amphiphysin II participates in the HCV life cycle by modulating the phosphorylation of NS5A.

Keywords: Proteome; NS5A; HCV; Amphiphysin II; Phosphorylation

Chronic infection with hepatitis C virus (HCV) carries with it a substantial risk of severe liver conditions such as chronic hepatitis, liver cirrhosis, and hepatocellular carcinoma. The interactions between cellular proteins and HCV gene products may provide clues for novel approaches to interfere with viral propagation and the accompanying pathogenesis. NS5A is a non-structural HCV protein thought to confer resistance to IFN therapy in HCV infection [1,2]. The NS5A protein in certain HCV isolates associates with IFN-induced double-stranded RNA-activated protein kinase (PKR) and inhibits PKR activity [3,4]. In addition, PKR-independent repression of IFN activity by NS5A, such as via the induction of IL-8 transcription, has been reported [5]. Several investigators have examined the role of NS5A in IFN resistance in vivo and in vitro, and have suggested the possibility that the number of mutations in the ISDR of NS5A is related to IFN responsiveness [1–4]. Thus, NS5A could be an important protein for the development of therapies against HCV infection.

The NS5A protein has been reported to interact with Grb2, p53, Cdk1, Pitx1, TRAF-2, karyopherin β3, and the SNARE-like protein, hVAP-33 (the human homologue of the 33-kDa vesicle-associated membrane protein-associated protein) [6–13]. To assess the effect of NS5A on cell function, it is important to identify proteins that interact

☆ *Abbreviations:* NS5A, hepatitis C virus non-structural protein 5A; ISDR, interferon sensitivity determining region; SH3, Src homology region 3; PAGE, polyacrylamide gel electrophoresis; LC–MS/MS, liquid chromatography–mass spectrometry/mass spectrometry.

* Corresponding author. Fax: +81 425 65 3315.
E-mail address: amasumi@nih.go.jp (A. Masumi).

0006-291X/$ - see front matter © 2005 Elsevier Inc. All rights reserved.
doi:10.1016/j.bbrc.2005.08.142

with NS5A. In the present study, we investigated NS5A-protein binding by a protein–protein interaction assay using cultured cells. Using LC–MS/MS analysis, we identified amphiphysin II as an NS5A-interacting protein in HeLa cells transfected with NS5A. Amphiphysin II has been reported to interact with c-myc and thereby possess anti-oncogenic function [14]. Zech et al. [15] previously identified amphiphysin II as an NS5A-interacting protein using an in vitro GST pull-down assay and demonstrated that IFN-α treatment abrogated this interaction by reducing NS5A levels in a HuH7 replicon system. However, the effect of this interaction on cellular function was not explored. Here, we determined the consequences of NS5A–amphiphysin II interactions for NS5A phosphorylation in vitro. NS5A is known to be the only phosphoprotein among the HCV non-structural proteins [16,17] and its hyperphosphorylation inhibits HCVRNA replication [18,19]. We demonstrated that its interaction with amphiphysin II reduces NS5A phosphorylation, which may help explain the mechanisms by which host defenses interact with the HCV during its life cycle.

Materials and methods

Cell lines and reagents. HeLa S3, HuH7, and 293T cells were cultured in Dulbecco's modified Eagle's medium (Sigma) supplemented with 10% fetal bovine serum, 2 mM L-glutamine, 100 U/ml penicillin, and 100 μg/ml streptomycin. Human IFN-α was purchased from Toray Co. Ltd.

Plasmid construction and stable transfectant production. Wild type NS5A cDNA was constructed from NIHJ1 (mutant NS5AcDNA) by modifying the ISDR [20,21]. Wild type and mutant NS5AcDNA were inserted into the *Hin*dIII–*Kpn*I sites of a p3×FLAG-CMV-14 expression vector (Sigma). The wild type NS5A expression vector (designated p5AFLAG) was transfected into HeLa S3 cells using Fugene6 (Roche Biochemicals) and after 2-weeks' culture with G418 (500 μg/ml), drug-resistant HeLa cells were pooled as stably transfected cells. Wild type HA-amphiphysin II cDNA and HA-amphiphysin II Δ10 cDNA (amphiphysin II lacking exon 10) were constructed from the amphiphysin II cDNA and subcloned into the *Bam*HI–*Xba*I sites of the pcDNA3.1(+) vector (Invitrogen) [22]. HA-amphiphysin II ΔSH3 cDNA was subcloned into the *Bam*HI–*Xho*I site of the pcDNA3.1(+) vector. The amphiphysin II mutants amphiphysin II Δ10, amphiphysin II ΔSH3, and amphiphysin II ΔN lacked the amino acids 250–266, 377–451, and 1–47, respectively [22].

Analysis by LC–MS/MS. HeLa cells stably transfected with NS5A-flag expression vector (p5AFLAG) were cultured in a 1 L spinner flask for 5 days. Cell extracts from HeLa cells were incubated with anti-flag M2-agarose and washed, and bound products were then eluted with flag peptide (0.2 mg/ml). The eluted fraction was electrophoresed on SDS–10% PAGE and stained with Silver Quest (Invitrogen). Individual protein bands were excised from the silver-stained gel and destained with a solution of 30 mM potassium ferricyanide/100 mM sodium thiosulfate (1:1) (v/v). Trypsin-digested sample solutions were analyzed by LC–MS/MS.

Preparation of cell extracts, M2-agarose, and HA-agarose pull-down assay, and Western blot analysis. 293T cells were transfected with full length amphiphysin II pcDNA3.1, amphiphysin II Δ10 pcDNA3.1, amphiphysin II ΔSH3 pcDNA3.1 or amphiphysin II ΔN pcDNA3.1 together with p5AFLAG. The transient transfection of 293T cells was carried out with Fugene 6 (Roche Biochemicals). The cells were harvested, washed with PBS, and lysed in lysis buffer M containing 50 mM Tris–HCl (pH 8.0), 100 mM NaCl, 0.1% NP-40, 1 mM EDTA, 1 mM dithiothreitol, and protein inhibitor cocktail (Sigma). Total cell lysates were incubated with M2-agarose (Sigma) or HA-agarose (Sigma) for 2 h on a rotator at 4 °C. After washing the agarose with lysis buffer M three times, the bound proteins were eluted with 0.2 mg/ml flag peptide (Sigma) or 1 mg/ml HA peptide (Sigma), and subjected to electrophoresis on SDS–10% PAGE, and analyzed by Western blotting with anti-flag (Sigma), anti-IRF-3 (Santa Cruz), anti-nucleolin (Santa Cruz), anti-stat1(UBI), anti-amphiphysin II(UBI), anti-c-Src (Santa Cruz), and anti-NS5A (Austral Biologicals) antibodies. The proteins were visualized by Chemiluminescence (Perkin Elmer).

In vitro kinase assays. Lysate from p5AFLAG and HA-amphiphysin II pcDNA3.1 cotransfected cells was incubated with anti-flag M2-agarose, and then the washed precipitate was reacted in kinase buffer (20 mM Tris–HCl, pH 8.0, 10 mM $MgCl_2$, and 1 mM Na_3VO_4) and 2 μCi, 10 μM [γ-^{32}P]ATP (Amersham) for 30 min at 37 °C. The reaction was terminated by the addition of an SDS sample buffer and boiling for 5 min at 95 °C, followed by SDS–10% PAGE and autoradiography.

Results

NS5A associates with amphiphysin II in HeLa cells

HeLa cells were stably transfected with p5AFLAG encoding NS5A conjugated with flag in the C-terminal domain. Expression of NS5A protein was confirmed by an anti-flag M2-agarose pull-down assay (Fig. 1A). Western blotting using anti-flag and anti-NS5A antibodies confirmed the production of flag-tagged NS5A protein in HeLa cells (Fig. 1A). To isolate proteins that associate with NS5A protein, cell lysate from a large-scale HeLa cell culture was incubated with anti-flag M2-agarose, and then the M2-agarose precipitate was eluted with flag peptide. The eluted fraction was electrophoresed and stained with silver. We observed that three bands a, b, and c increased compared to the level in the control (empty vector transfected) (Fig. 1B, lanes 1 and 2). These bands were cut out of the gel and digested with trypsin, and then the peptides were identified by LC–MS/MS. LC–MS/MS analysis identified band a as NS5A and band b as muscle type amphiphysin II [22]. Band c included β-tubulin, which was later identified as a non-specific protein. We focused on band b as an NS5A interaction protein. The indicated peptide coverage identified by LC–MS/MS for band b was approximately 42% (Fig. 1C). Western blot analysis using the amphiphysin II antibody confirmed that anti-flag M2-agarose precipitated amphiphysin II from HeLa cells transfected with p5AFLAG, but not control cells (Fig. 1D), further suggesting that amphiphysin II was specifically recruited to NS5A. We observed two bands by Western blotting which seemed to be phosphorylated and non-phosphorylated forms of amphiphysin II (Fig. 1D, top panel).

Several investigators have suggested that ISDR mutations in NS5A may be related to IFN responsiveness [1–4]. To examine whether the ISDR is important for interaction with amphiphysin II, an NS5A mutant NIHJ1-flag plasmid (with the ISDR modified as described previously) [20,21] was transfected together with HA-amphiphysin II pcDNA3.1 into 293T cells. Cell lysates were incubated with M2-agarose or HA-agarose, and then resin-bound products were eluted with flag peptide or HA peptide. As shown in Fig. 2, both wild type and mutant NS5A-bound

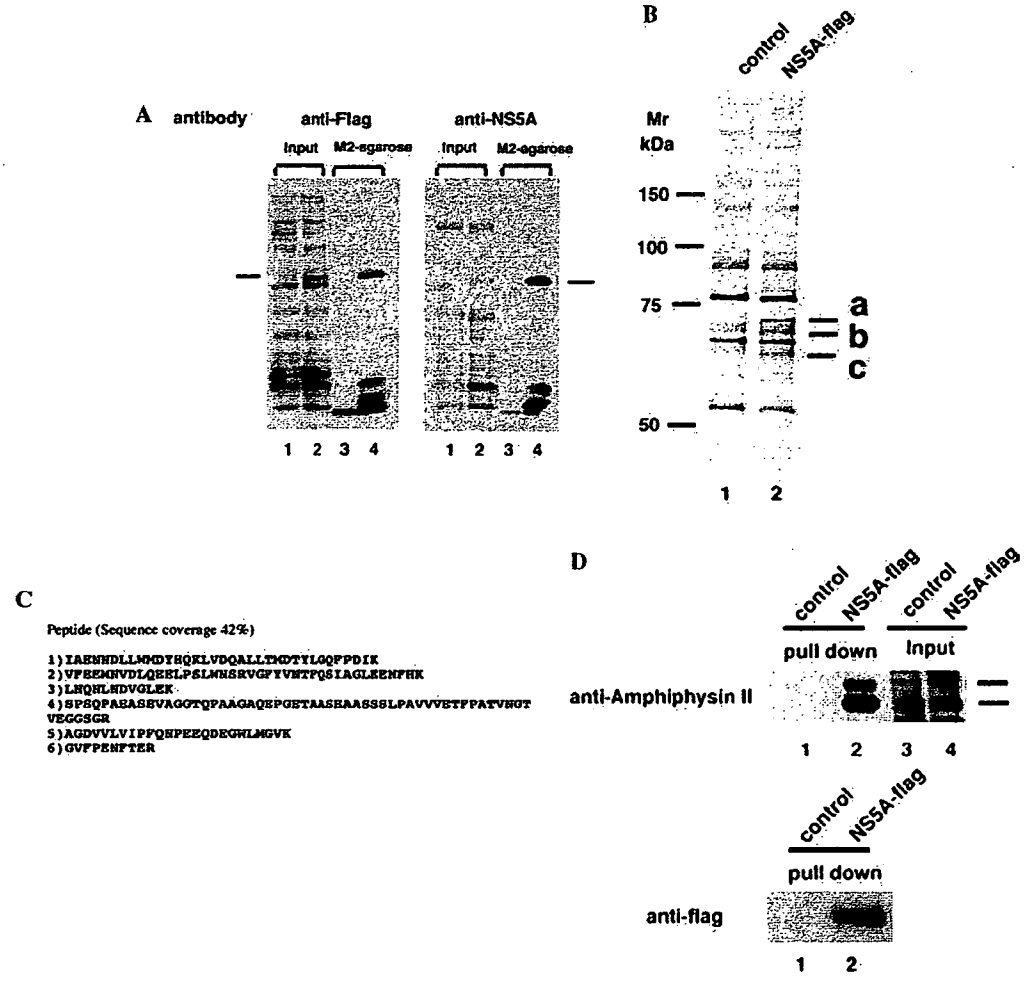

Fig. 1. Amphiphysin II associates with NS5A. (A) Expression of NS5A-flag protein in HeLa cells. NS5A-flag expression vector (p5AFLAG) (lanes 2 and 4) and a control vector (lanes 1 and 3) were transfected into HeLa cells. After a 2-week culture with geneticin 500 μg/ml, surviving cells were collected and lysed in lysis buffer. Cell lysate (lanes 1 and 2) was incubated with anti-flag M2-agarose and eluted with flag peptide (lanes 3 and 4) and then the eluate was subjected to Western blotting with anti-flag (left panel) or anti-NS5A (right panel) antibodies. (B) Cell lysates from large-scale (1 L) HeLa culture transfectants were incubated with anti-flag M2-agarose and then the flag peptide-eluted fractions from control and NS5A-transfectants were electrophoresed. Individual bands were analyzed by LC–MS/MS to identify proteins. The bands which are present in lane 2 but not lane 1 are indicated as a, b, and c. (C) Peptide coverage from trypsinized protein band b analyzed by LC–MS/MS. LC–MS/MS analysis identified band b as amphiphysin II. (D) Western blot analysis of M2-agarose immunoprecipitates. Anti-flag M2-agarose immunoprecipitates from control (lane 1) and NS5A-flag HeLa transfectants (lane 2) were electrophoresed and immunoblotted with anti-amphiphysin II and anti-flag antibodies. Aliquots of whole cell lysates from control cells (lane 3) and NS5A-flag transfectants (lane 4) were immunoblotted with the anti-amphiphysin II antibody.

amphiphysin II comparably, suggesting that the NS5A–amphiphysin II interaction is independent of the ISDR.

Next, we investigated the association of various proteins by Western blotting. As shown in Fig. 3A, c-Src protein was detected in anti-flag M2-agarose precipitates from HeLa cells transfected with p5AFLAG. IRF-3 and nucleolin were not detected as NS5A-interacting proteins, although these proteins are abundant in HeLa cells. Furthermore, in our system, we could not detect PKR or Pitx1 by Western blot analysis, although other investigators have reported that these proteins interact with NS5A [11] (data not shown).

We studied whether IFN-α treatment affects the interaction of NS5A with amphiphysin II or c-Src. Interestingly, IFN-α treatment reduced the c-Src–NS5A interaction, but not the amphiphysin II–NS5A interaction, although the expression of c-Src and amphiphysin II was unchanged after IFN-α treatment (Fig. 4). In a control experiment, Stat1 did not interact with NS5A before or after IFN-α treatment (Fig. 4). These results show that c-Src may be related to IFN-α-signaling factors, and that the interaction of amphiphysin II and NS5A is independent of the IFN-α response.

The interaction with amphiphysin II SH3 inhibits NS5A phosphorylation

To examine which region of amphiphysin II associates with NS5A, several amphiphysin II mutants were cotransfected into 293T cells with p5AFLAG. An anti-flag M2-

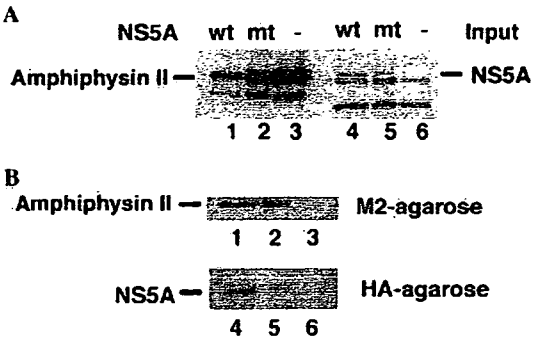

Fig. 2. NS5A associates with amphiphysin II in 293T cells. (A) p5AFLAG (lanes 1 and 4) or p5AFLAG mutant (NIHJ1 expression vector) (lanes 2 and 5) with HA-amphiphysin II pcDNA3.1 or only HA-amphiphysin II pcDNA3.1 (lanes 3 and 6) was transfected into 293T cells. Cell lysate from 293T cells was electrophoresed and immunoblotted with anti-amphiphysin II antibody (lanes 1–3) or anti-NS5A antibody (lanes 4–6). (B) Half of the cell lysate from 293T cells transfected with plasmids encoding wild type (lanes 1 and 4) or mutant NS5A (lanes 2 and 5) with HA-amphiphysin II pcDNA3.1 or only HA-amphiphysin II pcDNA3.1 (lanes 3 and 6) was incubated with anti-flag M2-agarose (lanes 1–3), and washed, and then the flag peptide-eluted fraction was immunoblotted with the anti-amphiphysin II antibody. The other half of the same 293T cell lysate was incubated with HA-agarose, and washed, and then the HA peptide-eluted fraction was immunoblotted with the anti-NS5A antibody (lanes 4–6).

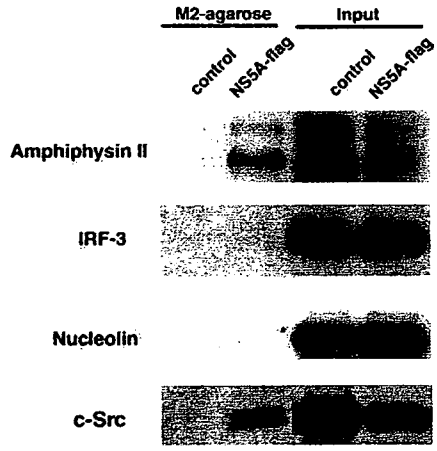

Fig. 3. Western blot analysis of NS5A-associated proteins in HeLa transfectants. Cell lysate from p5AFLAG-transfected HeLa cells was prepared, and then the flag peptide-eluted fraction from anti-flag M2-agarose immunoprecipitates was immunoblotted with anti-IRF-3, anti-nucleolin, and anti-c-Src, as well as anti-amphiphysin II antibodies.

agarose pull-down assay indicated that the amphiphysin II isoform Δ10 associated with NS5A, although the binding affinity was lower than with wild type (Fig. 5A). We also tested amphiphysin II ΔN, which is defective in the N-terminal region, and amphiphysin II ΔSH3, lacking the C-terminal region, for interaction with NS5A protein. As shown in Fig. 5B, NS5A associated with amphiphysin II ΔN to the same extent as with wild type amphiphysin II, but the association of amphiphysin II ΔSH3 with NS5A was markedly reduced. Together, these data suggest that the SH3 region of amphiphysin II is important for interacting with NS5A.

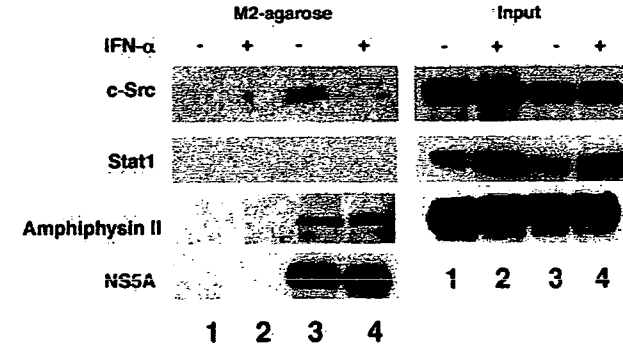

Fig. 4. IFN-α treatment inhibits the c-Src–NS5A interaction, but not the amphiphysin II–NS5A interaction. The M2-agarose pull down (left) and input (right) fractions were prepared from control HeLa cells (lanes 1 and 2) and HeLa–NS5A transfectants (lanes 3 and 4), untreated (lanes 1 and 3) or treated (lanes 2 and 4) with IFN-α (1000U) for 24 h. Immunoblot analysis was performed using anti-c-Src, anti-Stat1, anti-amphiphysin II, and anti-NS5A antibodies.

NS5A is known to be a phosphoprotein [17,23]. We investigated the effect of interaction of amphiphysin II with NS5A on phosphorylation of the latter. Anti-flag M2-agarose precipitates from 293T cells double-transfected with p5AFLAG and HA-amphiphysin II pcDNA3.1 were reacted in a kinase buffer containing [γ-^{32}P]ATP followed by immunoblotting with an anti-flag antibody. When HA-agarose precipitates from 293T cells double-transfected with p5AFLAG and HA-amphiphysin II pcDNA3.1 were immunoblotted with an anti-flag antibody, we detected a strong association of NS5A with wild type amphiphysin II, but not amphiphysin II ΔSH3 (Fig. 5C, top). As shown in Fig. 5C, NS5A from the M2-agarose precipitates were phosphorylated in vitro, suggesting that intracellular kinase associates with NS5A. NS5A from p5AFLAG and amphiphysin II pcDNA3.1 double-transfected 293T cells was much less phosphorylated than that from cells transfected with p5AFLAG alone (Fig. 5C, bottom). Amphiphysin II protein from HA-agarose precipitates of these double-transfected cells was also incubated in a kinase buffer, but amphiphysin II phosphorylation was not detectable (data not shown). We also tested NS5A phosphorylation using a human hepatic cell line, HuH7, because HCV is known to mainly infect hepatocytes [3]. HuH7 cells were double-transfected with p5AFLAG and amphiphysin II pcDNA3.1, and anti-flag M2-agarose precipitates were phosphorylated in vitro. We also detected NS5A phosphorylation in p5AFLAG and control vector-transfected HuH7 cells; however, NS5A from p5AFLAG and amphiphysin II pcDNA3.1-transfected HuH7 was much less phosphorylated (Fig. 5D). In addition, amphiphysin II ΔSH3 pcDNA3.1 transfection did not affect NS5A phosphorylation in HuH7 cells as in 293T cells (Figs. 5C and D). Here, we observed that HCV NS5A phosphorylation was regulated by host protein amphiphysin II. We conclude that the interaction between amphiphysin II and NS5A inhibits NS5A phosphorylation.

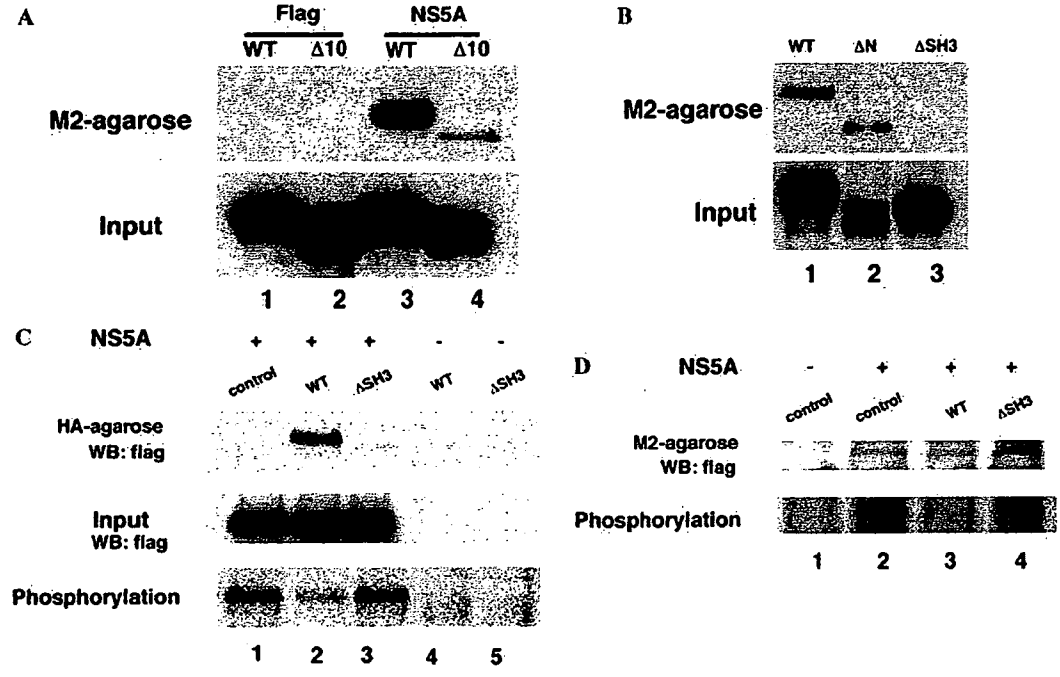

Fig. 5. NS5A associates with different amphiphysin II isoforms. (A) Full length amphiphysin II (lanes 1 and 3) or amphiphysin II Δ10 pcDNA3.1 (lanes 2 and 4) together with p5AFLAG were transfected into 293T cells and an anti-flag M2-agarose pull-down assay was performed. The flag peptide fraction was then immunoblotted with anti-amphiphysin II antibody. (B) Full length amphiphysin II (lane 1), amphiphysin II ΔN (lane 2), and amphiphysin II ΔSH3 (lane 3) deletion mutant plasmids were transfected into 293T cells with p5AFLAG and an anti-flag M2-agarose pull-down assay was performed. Then the flag peptide fraction was immunoblotted with anti-amphiphysin II antibody. (C) Amphiphysin II interaction inhibits NS5A phosphorylation. Empty vector pcDNA3.1 (lane 1), amphiphysin II pcDNA3.1 (lanes 2 and 4), amphiphysin II ΔSH3 pcDNA3.1 (lanes 3 and 5), and p5AFLAG (lanes 1–3) were transfected into 293T cells and half of the lysate was incubated with anti-flag M2-agarose while the other half was incubated with HA-agarose. The washed agarose was incubated with kinase reaction mixture containing [γ-^{32}P]ATP, boiled in an SDS-sample buffer, electrophoresed, and subjected to immunoblotting with anti-flag antibody (top and middle panels) or autoradiography (bottom panel). (D) Empty vector pcDNA3.1 (lanes 1 and 2), amphiphysin II pcDNA3.1 (lane 3), amphiphysin II ΔSH3 pcDNA3.1 (lane 4), and p5AFLAG (lanes 2–4) were transfected into HuH7 cells and the whole cell lysate was incubated with anti-flag M2-agarose. The washed agarose was incubated with kinase reaction mixture containing [γ-^{32}P]ATP, boiled in SDS-sample buffer, electrophoresed, and subjected to immunoblotting with the anti-flag antibody (top panel) or autoradiography (bottom panel).

Discussion

In this study, we demonstrated that HCV protein NS5A binds amphiphysin II in mammalian cells and that this interaction down-regulates NS5A phosphorylation, which affects the HCV life cycle. Amphiphysin II function was initially identified based on its ability to interact with c-myc and inhibit malignant transformation by this oncogene [14,24]. Amphiphysin II has several isoforms [22,25] and muscle type amphiphysin II is ubiquitously expressed amongst isoforms which localize to the cytoplasm and nucleus, and which is known to activate a caspase-independent apoptotic process [14,22]. Although widely expressed in normal cells, amphiphysin II is reported to exist in a functional form in ~50% of carcinoma cell lines and primary breast carcinomas examined. It should be noted that the amphiphysin II isoform in HeLa cells has been reported to be an exon 10-defective type [26]. Wild type amphiphysin II, which has exon 10, is a differentiation-associated isoform. In contrast, the amphiphysin II Δ10 isoform, which lacks exon 10, is involved in cell growth [26]. Although we found amphiphysin II as an NS5A-associated protein in HeLa cells, amphiphysin II–NS5A interactions in normal or non-transformed cells remain to be confirmed.

Zech et al. [15] reported that amphiphysin II and NS5A interact in HuH7 cells and showed that the binding of amphiphysin II to GST-NS5ApolyP-mutant fusion protein was reduced, while a NS5A C-terminal deletion mutant was completely unable to bind to amphiphysin II. Macdonald et al. [27] demonstrated that two closely spaced Class II polyproline motifs near the C-terminus of NS5A were able to bind isolated SH3 domains of Src kinase family members in vitro. Using Huh7-derived cells harboring sub-genomic HCV replicons, they showed that the expression of NS5A could differentially regulate the activity of endogenous Src family kinases and perturb Src-family-regulated-signaling pathways. However, their study found that NS5A in HuH7 cells did not bind GST-SrcSH3 [27]. In our report, c-Src was found to be an NS5A-associated protein in HeLa cells, although Src peptide fragments were not detected by LC–MS/MS analysis. c-Src can perhaps bind NS5A somewhere other than the SH3 region.

The ISDR of NS5A has been reported to be important for the IFN-α response [1,2,28]. We detected comparable affinity for amphiphysin II binding between the wild type

and ISDR mutant NS5A (Fig. 1), suggesting that NS5A ISDR is not critical for NS5A–amphiphysin II interactions. In our study, IFN-α treatment inhibited c-Src association with NS5A, while in contrast the binding affinity of amphiphysin II to NS5A did not change (Fig. 3). Dumenil et al. [29] reported that IFN-α inhibits the Src-mediated pathway necessary for *Shigella*-induced cytoskeletal rearrangement in epithelial cells. Our results suggest the possibility of an interaction between IFN signaling and the Src-mediated pathway, and appear to indicate that amphiphysin II association with NS5A does not affect the IFN-signaling pathway.

Both NS5A and amphiphysin II are known to be phosphoproteins [15,23,30]. NS5A has been reported to be phosphorylated by cAMP-dependent protein kinase and casein kinase II [31,32]. We observed that the phosphorylation of NS5A was reduced on interaction with amphiphysin II in both 293T and HuH7 cells. Phosphorylation of NS5A was not inhibited in the presence of amphiphysin II ΔSH3, which did not bind to NS5A. The interaction between amphiphysin II and NS5A is important for the inhibition of NS5A phosphorylation, although it is not yet clear how the SH3 region of amphiphysin II mechanistically affects the NS5A phosphorylation sites.

Recently, Neddermann et al. [18] demonstrated that hyperphosphorylation of NS5A inhibits HCV RNA replication. Evans et al. [19] reported that NS5A hyperphosphorylation disrupts interaction with hVAP-A and negatively regulates viral RNA replication. In our study, amphiphysin II expression reduced NS5A phosphorylation in a hepatic cell line, HuH7, which suggests that it may induce HCV RNA replication in HCV-infected cells. However, it is not yet known whether NS5A phosphorylation affects the interaction with amphiphysin II. HCV is known to mainly infect hepatocytes [3]. NS5A may bind amphiphysin II in normal hepatocytes and thus induce the transformation of these cells into hepatocellular carcinoma by inhibiting the anti-oncogenic function of amphiphysin II. It is as yet unclear how NS5A phosphorylation affects cellular transformation. The NS5A–host protein interaction affects both host defense and critical steps in the HCV life cycle such as viral replication. Such information as presented here on the interaction of NS5A and amphiphysin II should contribute to a better understanding of the mechanisms of host defense against HCV, and thus facilitate the development of effective anti-HCV therapies.

Acknowledgments

This work was supported by the Japan Health Sciences International Foundation and the Japan Society for Promotion of Sciences and the Ministry of Education, Science, Sports and Culture. We thank Drs. K.Takei, M. Kohase, Y. Aoki, S. Yamagoe, and Y. Murakami for useful discussions and Drs. T. Yoneyama, Y. Uehara, T. Miyamura, and K. Yamaguchi for generous support.

References

[1] N. Akuta, F. Suzuki, A. Tsubota, Y. Suzuki, T. Hosaka, T. Someya, M. Kobayashi, S. Saitoh, Y. Arase, K. Ikeda, H. Kumada, Association of amino acid substitution pattern in nonstructural protein 5A of hepatitis C virus genotype2a low viral load and response to interferon monotherapy, J. Med. Virol. 69 (2003) 376–383.

[2] S. Nishiguchi, T. Ueda, T. Ito, M. Enomoto, M. Tanaka, N. Tatsumi, K. Fukuda, A. Tamori, D. Habu, T. Takeda, S. Otani, S. Shiomi, Method to detect substitutions in the interferon-sensitivity-determining region of hepatitis C virus 1b for prediction of response to interferon therapy, Hepatology 33 (2001) 241–247.

[3] M.S. De Mitri, G. Morsica, R. Cassini, S. Bagaglio, M. Zoli, A. Alberti, M. Bernardi, Prevalence of wild-type in NS5A-PKR protein kinase binding domain in HCV-related hepatocellular carcinoma, J. Hepatol. 36 (2002) 116–122.

[4] J.R. Gale, M.J. Korth, N.M. Tang, S.-L. Tan, D.A. Hopkins, T.E. Dever, S.J. Polyak, D.R. Gretch, M.G. Katze, Evidence that hepatitis C virus resistance to interferon is mediated through repression of PKR protein kinase by the nonstructural 5A protein, Virology 230 (1997) 217–227.

[5] S. Polyak, K.S. Khabar, D.M. Paschal, H.J. Ezelle, G. Duverlie, G.N. Barber, D.E. Levy, N. Mukaida, D.R. Gretch, Hepatitis C virus nonstructural 5A protein induces interleukin-8, leading to partial inhibition of the interferon-induced antiviral response, J. Virol. 75 (2001) 6095–6106.

[6] S.-L. Tan, H. Nakao, Y. He, S. Vijayri, P. Neddermann, B.L. Jacobs, B.J. Mayer, M.G. Katze, NS5A, a nonstructural protein of hepatitis C virus virus, binds growth factor-bound protein 2 adaptor protein in a Src homology 3 domain/ligand-dependent manner and perturbs mitogenic signaling, Proc. Natl. Acad. Sci. USA 96 (1999) 5533–5538.

[7] K.H. Lan, M.L. Sheu, S.J. Hwang, S.H. Yen, S.Y. Chen, J.C. Wu, Y.J. Wang, N. Kato, M. Omata, F.Y. Chang, S.D. Lee, HCV NS5A interacts with p53 and inhibits p53-mediated apoptosis, Oncogene 18 (2002) 4801–4811.

[8] I. Qadri, M. Iwahashi, F. Simon, Hepatitis C virus NS5A binds TBP and p53, inhibiting their DNA binding and p53 interactions with TBP and ERCC3, Biochim. Biophys. Acta 1592 (2002) 193–204.

[9] K.M. Chung, J. Lee, J.E. Kim, O.K. Song, S. Cho, J. Lim, M. Seedorf, B. Hahm, S.K. Jang, Nonstructural protein 5A of hepatitis C virus inhibits the function of karyopherin beta3, J. Virol. 74 (2000) 5333–5341.

[10] K. Park, S. Choi, D. Choi, J. Park, S. Yie, S. Lee, S. Hwang, Hepatitis C virus NS5A protein modulates c-Jun N-terminal kinase through interaction with tumor necrosis factor receptor-associated factor 2, J. Biol. Chem. 278 (2003) 30711–30718.

[11] A.K. Ghosh, M. Majumder, R. Steele, R. Ray, R.B. Ray, Modulation of interferon expression by hepatitis C virus NS5A protein and human homeodomain protein Pitx1, Virology 306 (2003) 51–59.

[12] H. Tu, L. Gao, S.T. Shi, D.R. Taylor, T. Yang, A.K. Mircheff, Y. Wen, A.E. Gorbalenya, S.B. Hwang, M.M. Lai, Hepatitis C virus RNA polymerase and NS5A complex with a SNARE-like protein, Virology 263 (1999) 30–41.

[13] L. Gao, H. Aizaki, J. He, M. Lai, Interactions between viral nonstructural proteins and host protein hVAP-33 mediate the formation of hepatitis C virus RNA replication complex on lipid raft, J. Virol. 78 (2004) 3480–3488.

[14] J.B. DuHadaway, D. Sakamuro, D.L. Ewert, G.C. Prendergast, Bin1 mediates apoptosis by c-Myc in transformed primary cells, Cancer Res. 61 (2001) 3151–3156.

[15] B. Zech, A. Kurtenbach, N. Krieger, D. Strand, S. Blencke, M. Morbitzer, K. Salassidis, M. Cotten, J. Wissing, S. Obert, R. Bartenschlager, T. Herget, H. Daub, Identification and characterization of amphiphysin II as a novel cellular interaction partner of the hepatitis C virus NS5A protein, J. Gen. Virol. 84 (2003) 555–560.

[16] K.E. Reed, J. Xu, C.M. Rice, Phosphorylation of the hepatitis C virus NS5A protein in vitro and in vivo: properties of the NS5A-associated kinase, J. Virol. 71 (1997) 7187–7197.
[17] L. Huang, E.V. Sineva, M.R. Hargittai, S.D. Sharma, M. Suthar, K.D. Raney, C.E. Cameron, Purification and characterization of hepatitis C virus non-structural protein 5A expressed in Escherichia coli, Protein Expr. Purif. 37 (2004) 144–153.
[18] P. Neddermann, M. Quintavalle, C. Di Pietro, A. Clementi, M. Cerretani, S. Altamura, L. Bartholomew, R. De Francesco, Reduction of hepatitis C virus NS5A hyperphosphorylation by selective inhibition of cellular kinases activates viral RNA replication in cell culture, J. Viol. 78 (2004) 13306–13314.
[19] M.J. Evans, C.M. Rice, S.P. Goff, Phosphorylation of hepatitis C virus nonstructural protein 5A modulates its protein interactions and viral RNA replication, Proc. Natl. Acad. Sci. USA 101 (2004) 13038–13043.
[20] H. Aizaki, Y. Aoki, T. Harada, K. Ishii, T. Suzuki, S. Nagamori, G. Toda, Y. Matsuura, T. Miyamura, Full-length complementary DNA of hepatitis C virus genome from an infectious blood sample, Hepatology 27 (1998) 621–627.
[21] H. Aizaki, S. Saito, T. Ogino, N. Miyajima, T. Harada, Y. Matsuura, T. Miyamura, M. Kohase, Suppression of interferon-induced antiviral activity in cells expressing hepatitis C virus proteins, J. Interferon Cytokine Res. 20 (2000) 1111–1120.
[22] D. Sakamuro, K.J. Elliott, R. Wechsler-Reya, G.C. Prendergast, Bin1 is a novel MYC-interacting protein with features of a tumour suppressor, Nat. Genet. 14 (1996) 69–77.
[23] K. Reed, C. Rice, Identification of the major phosphorylation site of the hepatitis C virus H strain NS5A protein as serine 2321, J. Biol. Chem. 274 (1999) 28011–28018.
[24] A. Pineda-Lucena, C.H. Arrowsmith, Letter to the Editor: 1H, 13C and 15N resonance assignments and secondary structure of the c-Myc binding domain (MBD) and the SH3 domain of the tumor suppressor Bin1, J. Biomol. NMR 19 (2001) 191–192.
[25] E. Lee, M. Marcucci, L. Daniell, M. Pypaert, O.A. Weisz, G.C. Ochoa, K. Farsad, M.R. Wenk, P. De Camilli, Amphiphysin 2 (Bin1) and T-tubule biogenesis in muscle, Science 297 (2002) 1193–1196.
[26] R.J. Wechsler-Reya, K.J. Elliott, G.C. Prendergast, A role for the putative tumor suppressor Bin1 in muscle cell differentiation, Mol. Cell. Biol. 18 (1998) 566–575.
[27] A. Macdonald, K. Crowder, A. Street, C. McCormick, M. Harris, The hepatitis C virus NS5A protein binds to members of the Src family of tyrosine kinases and regulates kinase activity, J. Gen. Virol. 85 (2004) 721–729.
[28] G.K. Geiss, V.S. Carter, Y. He, B.K. Kwieciszewski, T. Holzman, M.J. Korth, C.A. Lazaro, N. Fausto, R.E. Bumgarner, M.G. Katze, Gene expression of profiling of the cellular transcriptional network regulated by alpha/beta interferon and its partial attention by the hepatitis C virus nonstructural 5A protein, J. Virol. 77 (2003) 6367–6375.
[29] G. Dumenil, J.C. Olivo, S. Pellegrini, M. Fellous, P.J. Sansonetti, G.T. Nhieu, Interferon alpha inhibits a Src-mediated pathway necessary for *Shigella*-induced cytoskeletal rearrangements in epithelial cells, J. Cell Biol. 143 (1998) 1003–1012.
[30] G. Waris, A. Livols, V. Imbert, J.-F. Peyron, A. Siddiqui, Hepatitis C virus NS5A and subgenomic replicon activate NF-kB via tyrosine phosphorylation of IkB and its degradation by Calpain, J. Biol. Chem. 278 (2003) 40778–40787.
[31] Y. Ide, A. Tanimoto, Y. Sasaguri, R. Padmanabhan, Hepatitis C virus NS5A protein is phosphorylated in vitro by a stably bound kinase from HeLa cells and by cAMP-dependent protein kinase A-a catalytic subunit, Gene 201 (1997) 151–158.
[32] J. Kim, D. Lee, J. Choe, Hepatitis C virus NS5A protein is phosphorylated by casein kinase II, Biochem. Biophys. Res. Commun. 257 (1999) 777–781.

THE JOURNAL OF BIOLOGICAL CHEMISTRY VOL. 281, NO. 38, pp. 28113–28121, September 22, 2006

Ets-1-dependent Expression of Vascular Endothelial Growth Factor Receptors Is Activated by Latency-associated Nuclear Antigen of Kaposi's Sarcoma-associated Herpesvirus through Interaction with Daxx*

Received for publication, March 3, 2006, and in revised form, July 19, 2006 Published, JBC Papers in Press, July 20, 2006, DOI 10.1074/jbc.M602026200

Yuko Murakami[‡], Satoshi Yamagoe[‡1], Kohji Noguchi[‡], Yutaka Takebe[§], Naoko Takahashi[‡], Yoshimasa Uehara[‡], and Hidesuke Fukazawa[‡]

From the [‡]Department of Bioactive Molecules and [§]Laboratory of Molecular Virology and Epidemiology, AIDS Research Center, National Institute of Infectious Diseases, Tokyo 162, Japan

Vascular endothelial growth factor (VEGF) and its receptors are highly expressed in Kaposi's sarcoma (KS) lesion and play a key role in angiogenesis. Latency-associated nuclear antigen (LANA) of Kaposi's sarcoma-associated herpesvirus (KSHV/HHV8) has multiple functions related to viral latency and KSHV-induced oncogenesis. In this report, we have identified Daxx as a LANA-binding protein by co-immunoprecipitation analysis of HeLa cells stably expressing LANA. LANA associated with Daxx in a PEL cell line infected with KSHV. LANA and Daxx also bound *in vitro*, suggesting direct interaction. From the results of binding assays, a region containing the Glu/Asp-rich domain within LANA, and a central region including the second paired amphipathic helix within Daxx contributed to the interaction. To address the physiological significance of this interaction, we focused on a Daxx-mediated VEGF receptor gene regulation. We found that Daxx repressed Ets-1-dependent Flt-1/VEGF receptor-1 gene expression, and that LANA inhibited the repression by Daxx in a reporter assay. Analyses of flow cytometry and real-time PCR revealed that expression of VEGF receptor-1 and -2 in LANA-expressing human umbilical vein endothelial cells (HUVECs) significantly increased. Co-immunoprecipitation and immunoblotting experiments suggested that LANA-bound Daxx to inhibit the interaction between Daxx and Ets-1. Chromatin immunoprecipitation assays showed that Daxx associated with VEGF receptor-1 promoter in HUVECs, and that LANA expression reduced this association. These results suggested that LANA contributes to a high expression of VEGF receptors in KS lesion by interfering with the interaction between Daxx and Ets-1.

Kaposi's sarcoma-associated herpesvirus (KSHV[2]/HHV8) has been found to be the pathogen of Kaposi's sarcoma (KS) (1) (2), two B cell malignancies, primary effusion lymphoma (PEL), and multicentric Castleman's disease (MCD) (3). Among over 80 ORFs of KSHV (4), LANA (latency-associated nuclear antigen) is exceptionally highly expressed in KS lesion, PEL, and also in MCD (5) (3), so that LANA is used as a diagnostic marker of KSHV. LANA is reported to be a multifunctional protein that tethers its own viral episomal DNA to host chromosomes in mitosis to segregate KSHV into progeny cells (6) (7) and also binds many host molecules to regulate expression of cellular genes. LANA inhibits p53-induced apoptosis (8), transforms fibroblast by co-transfection with the Ras oncogene (9) and also stabilizes β-catenin to stimulate entry into S phase (10). LANA seems to contribute to pathogenesis of KSHV-associated malignancies through these interactions.

We identified Daxx as a new LANA-interacting host protein. To know the biological significance of the interaction between LANA and Daxx, we focused on Daxx-modulated transcription. Daxx was found initially as a Fas-binding protein to regulate apoptosis (11) and later reported to bind with several nuclear proteins and transcription factors. Daxx was shown to act as a transcriptional repressor of Ets-1 (12), Pax3 (13), Pax5 (14), and p53 (15) through protein-protein interaction. In the case of Ets-1, Daxx repressed Ets-1-dependent expression of matrix metalloproteinase 1 (MMP1) and Bcl-2 (12). Ets-1 belongs to the Ets family of transcriptional factors, and regulates various gene expressions through binding to a unique motif (GGAA) on their promoters. Ets-1 regulates genes related to angiogenesis: Flt-1/VEGF receptor-1, KDR/VEGF receptor-2, and matrix metalloproteinases (MMPs) (16). Ets-1 is specifically expressed in lymphoid tissues, endothelial cells (17), and also in the spindle cells of KS lesion, derived from endothelial origins (18). In KS lesion, angiogenic factors such as VEGF and VEGF receptors were highly expressed (1) (19). Vascular angiogenesis plays an important role in the development and progression of tumors, especially KS (20) (21) (22). We therefore examined the role of LANA in interaction between Daxx

* This work was supported in part by a grant for Research on Health Sciences focusing on Drug Innovation from The Japan Human Sciences Foundation. The costs of publication of this article were defrayed in part by the payment of page charges. This article must therefore be hereby marked "*advertisement*" in accordance with 18 U.S.C. Section 1734 solely to indicate this fact.

[1] To whom correspondence should be addressed: Dept. of Bioactive Molecules, National Institute of Infectious Diseases, Toyama 1-23-1, Shinjuku-ku, Tokyo, 162–8640, Japan. Tel.: 81-3-5285-1111; Fax: 81-3-5285-1272; E-mail: syamagoe@nih.go.jp.

[2] The abbreviations used are: KSHV, Kaposi's sarcoma-associated herpesvirus; VEGF, vascular endothelial growth factor; ORF, open reading frame; DTT, dithiothreitol; PMSF, phenylmethylsulfonyl fluoride; HA, hemagglutinin; GST, glutathione S-transferase; DAPI, 4′,6-diamidino-2-phenylindole; ChIP, chromatin immunoprecipitation assay; GFP, green fluorescent protein; PAH, paired amphipathic helix; HUVEC, human vascular endothelial cells; LANA, latency-associated nuclear antigen; aa, amino acids; Ets, E26 transformation-specific.

and Ets-1, and show here a possible new function of LANA on the expression of VEGF receptors.

EXPERIMENTAL PROCEDURES

Plasmids—LANA gene was cut from L54 Lambda FIX II vector (NIH AIDS Research & Reference Reagent Program), at the EheI site (123743 and 127293 of KSU75698) and inserted into the EcoRV site of pFLAG-CMV-2 expression vector (Sigma) to make an N-terminal FLAG-tagged LANA expression vector, pFLAG-LANA. For *in vitro* translation/transcription system, the *LANA* gene from pFLAG-LANA was subcloned between the EcoRI and KpnI sites of pBluescript II KS(+) plasmid after correction of the N-terminal 5 bases using synthetic oligonucleotides, 5′-AATTCATCGATGGCGCCCCCGGGAATGCG-3′ and 5′-CATTCCCGGGGGCTCTATCGATG-3′ (using EcoRI and BsmI sites), to obtain pBluescript-LANA. A series of C-terminal deletion mutants of LANA (L1 to L4) were constructed from pBluescript-LANA using an exonuclease III/mung bean deletion kit (Toyobo, Tokyo, Japan) according to the manufacturer's instructions. An N-terminal deletion mutant of LANA (L5) was constructed with pBluescript-LANA by cutting the N-terminal region at EcoRI and PstI sites and joining it with synthetic oligonucleotides, 5′-AATTCATCGATGGAGCCCCTGCA-3′ and 5′-GGGCTCCATCGATG-3′. PFLAG-LANA deletion mutants (pFLAG-LANA-N1 to pFLAG-LANA-C) were constructed with L1–L5 and pFLAG-CMV-2 vector. Full-length and various deletion mutants of the *Daxx* gene were generated by PCR amplification from cDNA of HeLa cells, subcloned into pCR-Blunt II-TOPO plasmid (Invitrogen, Carlsbad, CA), and cloned between the EcoRI and the SalI sites of pcDNA3.1 (−) (Invitrogen) (termed pcDNA-Daxx), pCMV-HA (Clontech Laboratories, Inc. Palo Alto, CA), or pGEX-6P-3 (Amersham Biosciences, Piscataway, NJ). A luciferase reporter plasmid, pFlt-1-luc (containing human Flt-1 promoter −748/+248, D64016) was kindly provided by Dr. K. Morishita (23). Human *ets-1* genes of p51Ets-1 and p42Ets-1 (the full-length Ets-1 and a variant lacking the regulatory domain, exon VII, respectively (24)), were cut from plasmids kindly provided by Dr. R. Li (12), and cloned into pcDNA3.1(+) (Invitrogen). The constructed plasmids were termed pcDNA-p51Ets-1 and pcDNA-p42Ets-1, respectively. For flow cytometric analysis, the full-length *LANA* gene from the pBluescript-LANA was cloned between the SacI and SalI sites of pIRES2-EGFP vector (Clontech), termed pIRES2-LANA-EGFP.

Cell Culture and Transfection—HeLa cells and human embryonic kidney 293T cells were cultured in Dulbecco's modified medium supplemented with 10% bovine fetal serum. A KSHV-infected PEL cell line, BCBL-1 cells (kindly provided by Dr. H. Katano) were cultured in RPMI 1640 with 10% bovine fetal serum. Human umbilical vein endothelial cells (HUVEC) (Clonetics, San Diego, CA) were cultured in EGM-2 medium (Clonetics). Transfection was performed with FuGENE6 (Roche Diagnostics, Indianapolis, IN) for HeLa and 293T cells or by Nucleofecter system (amaxa GmbH, Cologne, Germany) for HUVEC.

Identification of LANA-binding Protein—PFLAG-LANA was transfected into HeLa cells and stable LANA-expressing clones were selected. LANA-expressing cells of six liters were harvested, nuclear extract was prepared as previously described (25), and dialyzed against a buffer containing 20 mM Tris-HCl, pH 7.5, 100 mM NaCl, 0.2 mM EDTA, 10% glycerol, 1 mM phenylmethylsulfonyl fluoride (PMSF), and 10 mM β-mercaptoethanol. The nuclear extract was adjusted to 150 mM NaCl and 0.1% Tween 20 before absorption into anti-FLAG antibody (M2) affinity gel (Sigma). The gel was washed with 150 mM washing buffer (20 mM Tris-HCl, pH 8.0, 5 mM $MgCl_2$, 150 mM NaCl, 1 mM dithiothreitol (DTT), 10% glycerol, 1 mM PMSF), and eluted with the same buffer containing 200 μg/ml of FLAG peptides. The eluted protein was applied to SDS-PAGE and stained with Coomassie Brilliant Blue or silver stained. The Coomassie-stained band was cut and treated with lysyl endopeptidase. The extracted peptides were purified using HPLC, and analyzed with a Procise 494 HT Protein Sequencing System (Applied Biosystems, Foster City, CA).

Immunoprecipitation and Western Blotting—Cells were harvested and lysed with low salt buffer (10 mM HEPES, pH 7.9, 10 mM KCl, 1.5 mM $MgCl_2$, 1 mM DTT containing 0.5% Nonidet P-40, 1 mM PMSF, 25 μg/ml each of antipain, pepstatin, and leupeptin), then centrifuged to collect the nuclei. The nuclear pellet was lysed with nuclear extract buffer (20 mM Tris-HCl, pH 7.9, 5 mM, EDTA, 300 mM NaCl, 1 mM PMSF), and the same volume of distilled water was added. Nuclear extract was subjected to immunoprecipitation either with anti-FLAG antibody (M2), anti-Daxx antibody (sc-7152) (Santa Cruz Biotechnology, Inc., Santa Cruz, CA), or anti-Ets-1 antibody (Santa Cruz Biotechnology, sc-350). The immune complex was washed with 150 mM washing buffer, resolved in Laemmli's sample buffer and applied to SDS-PAGE. Proteins in gels were transferred to PVDF membrane followed by Western blotting using anti-FLAG antibody (M5, Sigma), anti-Daxx antibody (sc-7152), anti-LANA antibody (Advanced Biotechnologies, Columbia, MD), anti-Ets-1 antibody (sc-350), or anti-HA antibody (Sigma).

GST Pull-down Assay—Glutathione *S*-transferase (GST)-Daxx fusion proteins were expressed in *Escherichia coli*, and purified using affinity matrix glutathione-Sepharose beads (Amersham Biosciences). ^{35}S-labeled LANA was made *in vitro* with TnT quick-coupled reticulocyte transcription/translation systems (Promega, Madison, WI). GST-Daxx fusion proteins were bound to glutathione-Sepharose beads and incubated with the translated products containing ^{35}S-labeled LANA in binding buffer (25 mM HEPES, pH 7.6, 50 mM NaCl, 2.5 mM $MgCl_2$, 1 mM DTT, 0.05% Triton X-100, 1 mM PMSF) at room temperature for 15 min. After washing with washing buffer (25 mM HEPES, pH 7.6, 150 mM NaCl, 2.5 mM $MgCl_2$, 1 mM DTT, 0.5% Triton X-100, 1 mM PMSF), proteins adsorbed to the beads were resolved and applied to SDS-PAGE. Proteins in the gel were stained with Coomassie Brilliant Blue, and the radioactivity was detected by BAS-1500 (Fuji Film, Tokyo).

Immunofluorescence Assay—BCBL-1 cells were attached to slide glasses with a cell concentrator (StatSpin, Norwood, MA). HeLa cells were seeded on chamber slides (Lab-Tek, Campbell, CA). The cells were fixed in 4% paraformaldehyde in PBS(−), permeabilized with 0.2% Triton X-100, and incubated with anti-LANA antibody (Advanced Biotechnologies) (diluted to 1:500 or 1:1000) and anti-Daxx antibody (sc-7152) (diluted to

1:100 or 1:200) followed by fluorescent-conjugated second antibody (Alexa Fluor 488 anti-rat IgG and Alexa Fluor 594 anti-rabbit IgG, Molecular Probes, Eugene, OR) (diluted to 1:200 each). Cell nuclei were stained with DAPI in mounting oil (Vectashield with DAPI, Vector Laboratories, Burlingame, CA). Immunostained cells were analyzed by a confocal laser scanning microscope using a Carl Zeiss LSM510 system (Carl Zeiss, Oberkochen, Germany).

Transcriptional Reporter Assay—293T cells (2×10^5 cells/well) grown in 24-well plates were transfected with pFlt-1-luc, pRSV-β-Gal (for transfection efficiency), and the combination of pcDNA-p51Ets-1, pcDNA-p42Ets-1, pcDNA-Daxx, or pFLAG-LANA, with 2 μl of FuGENE6. Total DNA was adjusted to a constant amount (800 ng). Two days after transfection, the cells were lysed and applied to luciferase assay (Toyo Inki, Tokyo) and β-galactosidase enzyme assay system (Promega). Assays were performed in triplicate, and the experiments were repeated three times.

Flow Cytometric Analysis—HUVECs transfected with either pIRES2-LANA-EGFP or pIREAS2-EGFP as control, were subjected to FACS Vantage (Becton Dickinson, Franklin Lakes, NJ) to collect GFP-expressing cells 2 days after transfection. The GFP-expressing cells cultured for 10 days were incubated with anti-Flt-1 or anti-KDR antibody (V4262, V9134, respectively, Sigma) and PE-labeled secondary antibody (R0439, Dako Cytomation, Carpinteria, CA). The cells were analyzed by a FACS Calibur flow cytometer (Becton Dickinson).

Quantitative Real-time RT-PCR—HUVECs were transfected with either pIRES2-LANA-EGFP or pIREAS2-EGFP using Nucleofector system, and sorted with FACS Aria (Becton Dickinson) to collect GFP-expressing cells. Total RNA was extracted with RNeasy Mini kit (Qiagen GmbH, Hilden, Germany), and reverse-transcribed to cDNA with oligo(dT) by Superscript First-strand synthesis system according to the manufacturer's instructions (Invitrogen). The cDNA was applied to Real-Time PCR using SYBR Premix Ex Taq (Takara Bio Co.) with ABI PRISM7000 (Applied Biosystems). PCR was performed at 95 °C for 10 s, followed by 40 cycles of 95 °C for 5 s and 60 °C for 34 s. The primers were designed using software Primer Express (Applied Biosystems). The forward and reverse primers for Flt-1 were 5′-CCCTTATGATGCCAGCAAGTG-3′ and 5′-CCAAAAGCCCCTCTTCCAA-3′, respectively, and primers for KDR were 5′-CACCACTCAAACGCTGACATGTA-3′ and 5′-CCAACTGCCAATACCAGTGGAT-3′. Primers for Daxx were 5′-GCCCTTCACCACTGTCTTAGAGA-3′ and 5′-GAGACGCCTCCATTGAAGGA-3′. As an internal control, glyceraldehyde-3-phosphate dehydrogenase (GAPDH) was used with primers 5′-GGAGTCAACGGATTTGGTCGTA-3′, and 5′-GGCAACAATATCCACTTTACCAGAGT-3′. The primers for Ets-1 were 5′-CTGCGCCCTGGGTAAAGA-3′ and 5′-CCCATAAGATGTCCCCAACAA-3′. In the case of Ets-1, primers for GAPDH were 5′-CCACCCATGGCAAATTCC-3′ and 5′-TGGGATTTCCATTGATGACAAG-3′. Obtained data were analyzed according to the sequence detector program (Applied Biosystems).

Chromatin Immunoprecipitation (ChIP) Assay—ChIP assays were performed basically using a kit from Upstate Biotechnology (Lake Placid, NY) with some modifications. Cells (5×10^6 cells/assay) were treated with 1% formaldehyde for 5 min for

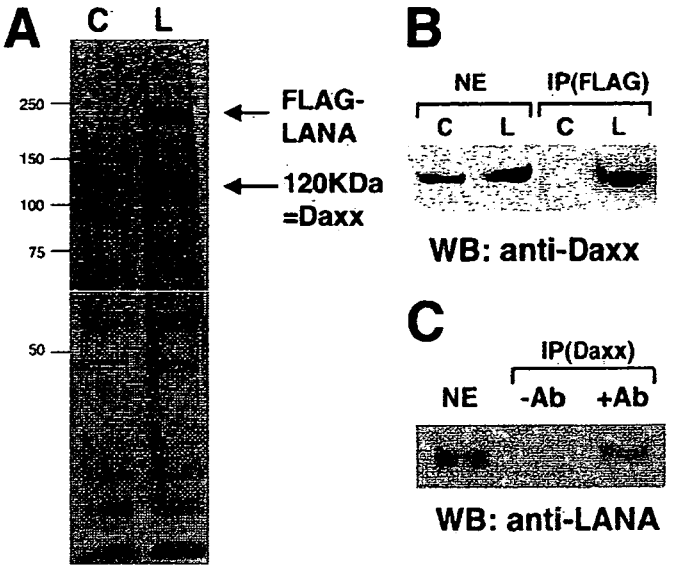

FIGURE 1. **Identification of Daxx as a LANA-binding protein.** *A*, immune complex with anti-FLAG antibody of nuclear extract (*NE*) of HeLa cells was analyzed by SDS-PAGE. Proteins were detected with silver staining. A protein of 120 kDa associated with FLAG-LANA was identified as Daxx. (*C*: control parent HeLa cells, *L*: LANA-expressing HeLa cells). *B*, immune complex with anti-FLAG antibody followed by Western blotting (*WB*) with anti-Daxx antibody. Daxx was detected at about 120 kDa. *C*, immune complex with anti-Daxx antibody followed by Western blotting with anti-LANA antibody using nuclear extract of BCBL-1 cells. A band of about 250 kDa was detected as LANA.

cross-linking, lysed with 400 μl of lysis buffer (10 mM HEPES, pH 7.9, 60 mM KCl, 0.5% Nonidet P-40, 1 mM PMSF, 25 μg/ml each of antipain, pepstatin, and leupeptin), and centrifuged to collect the nuclei. The nuclear pellet was lysed with 200 μl of SDS lysis buffer (50 mM Tris-Hcl, pH 8.1, 10 mM EDTA, 1% SDS), and sonicated 6 times for 30 s each time. Centrifuged supernatants were then diluted with 1.8 ml of ChIP dilution buffer (0.01% SDS, 1.1% Triton X-100, 1.2 mM EDTA, 16.7 mM Tris-HCl, pH 8.0), and precleared with protein A agarose/salmon sperm DNA. Anti-Ets-1 (Santa Cruz Biotechnology, sc-350), anti-Daxx antibody (Santa Cruz Biotechnology, sc-7152), or rabbit IgG (Sigma) as the negative control was added respectively to the supernatant, and rotated overnight at 4 °C. The mixture was then incubated with protein A-agarose/salmon sperm DNA for 1 h at 4 °C. The protein A-agarose-conjugated complex was washed, and DNA fragments were eluted and prepared according to the manufacturer's instructions. The prepared DNA was resolved in 20 μl of H_2O and 2 μl was used for PCR. Primers used were 5′-GGGACCCCTTGACGTCACCA-3′ (corresponding to −90 to −71 of Flt-1 promoter) and 5′-ACCTCGATGAAGAGCAGCCG-3′ (corresponding to −12 to +8 of Flt-1 promoter). Ex Taq polymerase (Takara Bio Co.) was used, and PCR conditions were 30 cycles of 94 °C for 30 s, 55 °C for 30 s and 72 °C for 30 s. The PCR products were analyzed on a 1.8% agarose gel.

RESULTS

Identification of Daxx as a LANA-binding Protein—To identify host proteins that associate with LANA, we constructed a plasmid expressing FLAG-LANA (N terminus-tagged) to transfect into HeLa cells and established several stable LANA-

expressing clones. We cultured one clone of the LANA-expressing cells and prepared nuclear extract. This extract was incubated with anti-FLAG affinity gel (M2-agarose), followed by elution with FLAG peptides. Eluate was subjected to SDS-PAGE to detect a prominent 120-kDa band (Fig. 1*A*). Although there was a 75-kDa band, which was a nonspecific binding protein commonly found with the antibody. We determined the sequences of the N-terminal 10 residues of the 120-kDa protein, which revealed the protein to be Daxx. To confirm the identification, the nuclear extract (each 500 μg of protein) was immunoprecipitated with anti-FLAG antibody to apply to immunoblotting with anti-Daxx antibody. As shown in Fig. 1*B*, anti-Daxx antibody recognized a band of 120 kDa. These results indicated that Daxx is a cellular binding protein of exogenously expressed LANA in the HeLa cell. To confirm LANA-Daxx interaction in a physiological context, we immunoprecipitated with anti-Daxx antibody from nuclear extracts of BCBL-1 cells, a PEL cell line infected with KSHV. LANA was co-immunoprecipitated with Daxx as well (Fig. 1*C*). This result suggested that LANA formed a complex with Daxx in KSHV-infected cells.

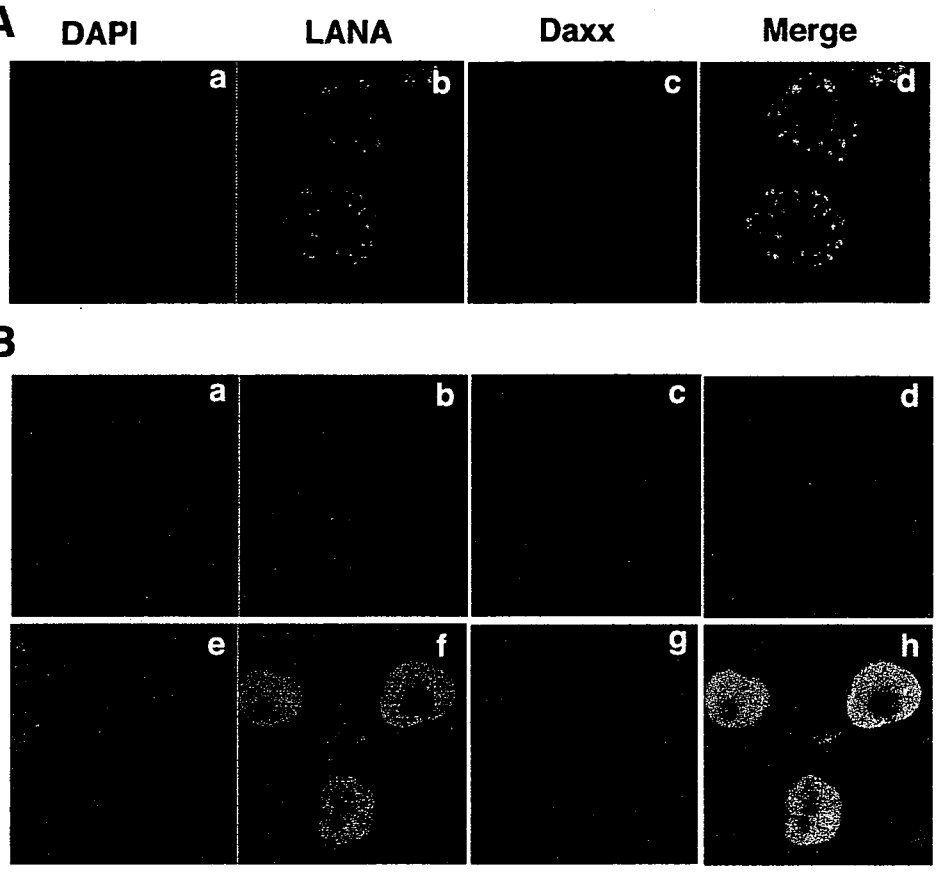

FIGURE 2. **LANA co-localizes with Daxx in BCBL-1 cells and HeLa cells.** Confocal microscopic images of PEL cell line, BCBL-1 cells (*A*), and HeLa cells (*B*, control (*panels a–d*) and LANA-expressing cells (*panels e–h*)). Cells were doubly immunostained with anti-LANA antibody (1:500 for *A*, 1:1000 for *B*) and anti-Daxx antibody (1:100 for *A*, 1:200 for *B*). Images represent cells stained with DAPI (*panels a* and *e*), anti-LANA antibody (*panels b* and *f*), or anti-Daxx antibody (*panels c* and *g*), and merged images of LANA and Daxx staining (*panels d* and *h*).

Colocalization of LANA and Daxx in the Nuclei of KSHV-infected Cell Line BCBL-1—Next we examined the localization of LANA and Daxx in BCBL-1 by immunofluorescence microscopic assay (Fig. 2*A*). LANA gave a characteristic speckled staining pattern in nuclei of the cells (Fig. 2*A*, *panel b*), Daxx also showed some speckles in the nuclei (Fig. 2*A*, *panel c*). The merged image indicated that LANA considerably co-localized with Daxx in the nuclear dots (Fig. 2*A*, *panel d*). We also investigated the localization of Daxx using HeLa cells (Fig. 2*B*). LANA gave fine patchy staining in the nucleus (Fig. 2*B*, *panel f*), which is a typical observation in the absence of KSHV genome (Fig. 2*B*, *panel g*). The parental HeLa cells showed diffused staining of Daxx throughout the cell (Fig. 2*B*, *panel c*). In contrast, Daxx appeared to accumulate in the nuclei of the LANA-expressing cells (used in Fig. 1) (Fig. 2*B*, *panel g*). LANA and Daxx largely localized in the nucleus of the HeLa cells (Fig. 2*B*, *panel h*). We performed biochemical fractionation using three independent clones of LANA-expressing HeLa cells and examined cellular localization of Daxx by Western blotting. The results indicated that the amount of Daxx in the nuclear fraction increased as LANA expression increased, although total amounts of Daxx were comparable in these HeLa clone cells (data not shown).

A Region Containing the Acidic-rich Domain in LANA Is Required for Binding with Daxx—To determine the interacting domain of LANA with Daxx, we constructed a series of LANA deletion mutants (Fig. 3*A*), which were translated *in vitro* and subjected to pull-down assay with GST-Daxx. As shown in Fig. 3*B*, full-length LANA was pulled down with GST-fused full-length Daxx, indicating direct interaction between LANA and Daxx. Three N-terminal mutants of LANA (L1–L3) bound with GST-Daxx, but the shortest N-terminal LANA (aa 1–261) (L4), and C-terminal LANA (aa 496–740) (L5) failed (Fig. 3*B*). We constructed mammalian expression plasmids, LANA-N (aa 1–564), LANA-C (aa 496–1162), LANA-N1 (aa 1–260), LANA-N2 (aa 1–320), LANA-N3 (aa 1–344), and LANA-ΔAD (with aa 322–493 deleted) (Fig. 3*A*). These plasmids were co-transfected with pcDNA-Daxx into 293T cells, and the nuclear extracts were analyzed. Immunoprecipitation with anti-Daxx antibody and Western blotting with anti-FLAG antibody indicated that Daxx formed a complex with full-length LANA and LANA-N, and weakly with LANA-N3, but not with the other LANA fragments (Fig. 3*C*). Taken together, these results suggested that aa 320–344 of LANA, which contains many aspartic acids and glutamic acids, were required for binding with Daxx.

A Central Domain of Daxx Is Required to Interact with LANA—To determine the critical region of Daxx for binding with LANA, a series of GST-fused deletion mutants of Daxx (Fig. 4*A*)

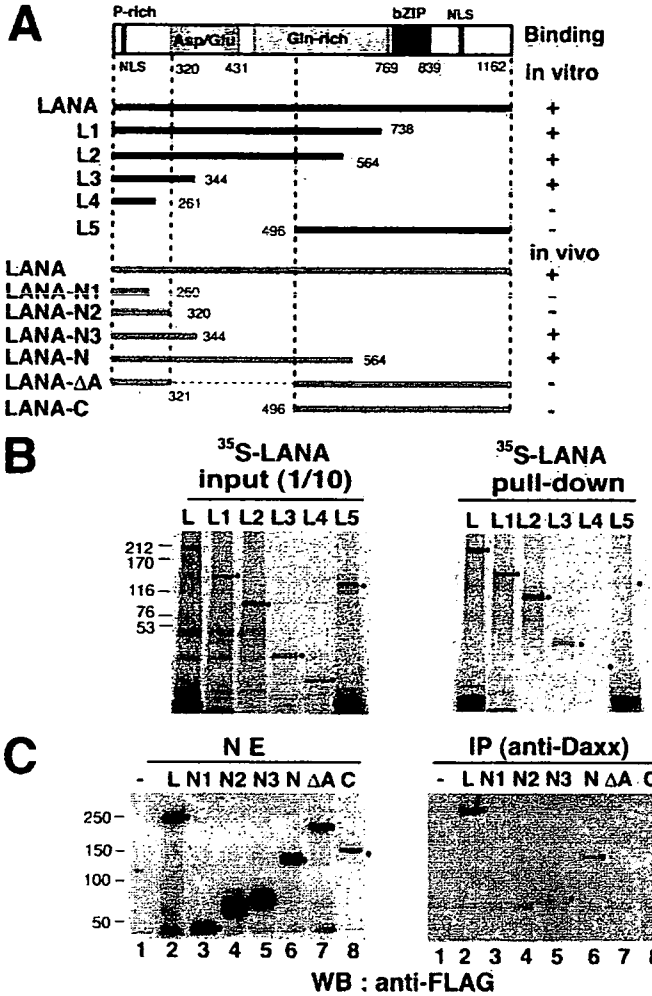

FIGURE 3. **A region containing an acidic-rich domain in LANA is required for binding with Daxx *in vitro* and *in vivo*.** *A*, domain structure of LANA and its deletion mutants. LANA is constituted of domains of proline-rich, acidic-rich, glutamine-rich, and basic leucine-zipper. A series of deletion mutants of LANA and the binding activity *in vitro* and *in vivo* are shown. *B*, result of pull-down assay with GST-fused full-length Daxx of ^{35}S-labeled LANA deletion mutants (*L1–L5*). *C*, co-immunoprecipitation of Daxx and LANA deletion mutants in 293T cells. PFLAG-CMV-2 vector (4.0 μg) (*lane 1*), pFLAG-LANA (4.0 μg) (*lane 2*), pFLAG-LANA-N1 (1.0 μg) (*lane 3*), pFLAG-LANA-N2 (2.0 μg) (*lane 4*), pFLAG-LANA-N3 (2.0 μg) (*lane 5*), pFLAG-LANA-N (2.0 μg) (*lane 6*), pFLAG-LANA-ΔA (4.0 μg) (*lane 7*), or pFLAG-LANA-C (4.0 μg) (*lane 8*) was individually co-transfected with pcDNA-Daxx (1.0 μg) in 60-mm dishes with adjustment of total DNA amount (5.0 μg). The immunoprecipitates (*IP*) with anti-Daxx antibody were followed by immunoblotting (*WB*) with anti-FLAG antibody (M5).

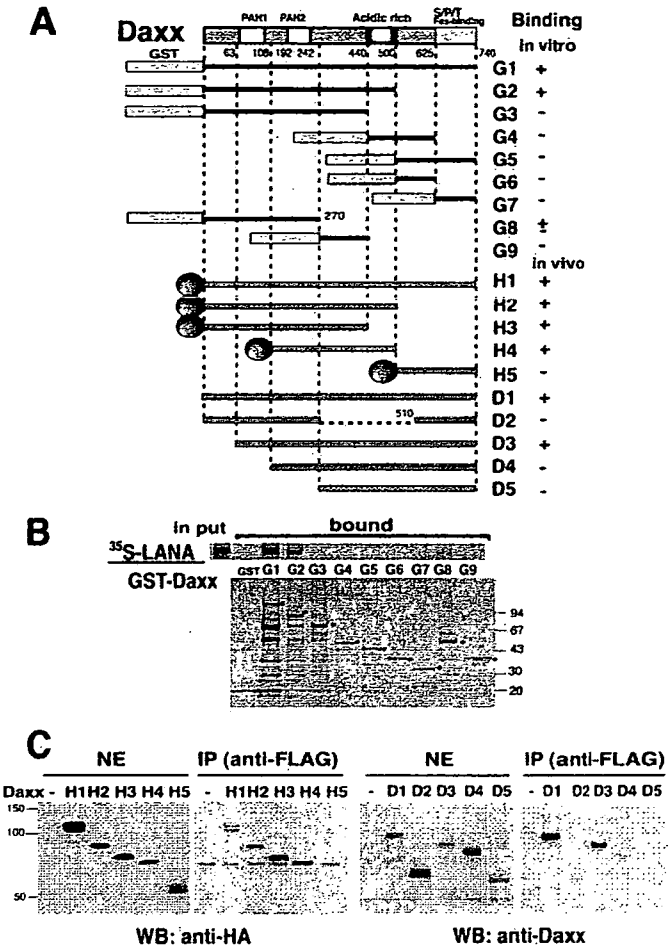

FIGURE 4. *A*, central region containing PAH 2 and acidic-rich domain in Daxx is required to interact with LANA. *A*, domain structure of Daxx and various deletion mutants. Daxx is composed of two PAH and acidic-rich and Ser/Pro/Thr-rich domains. A series of mutants of Daxx and the binding activity *in vitro* and *in vivo* are shown. *B*, purified GST-Daxx variants (*G1–G9*) were applied in *in vitro* pull-down assay with full-length ^{35}S-LANA. *C*, mammalian expression plasmids, pCMV-HA-Daxx-H1 (full-length) (2.0 μg), pCMV-HA-Daxx-H2 (aa 1–500) (2.0 μg), pCMV-HA-Daxx-H3 (aa 1–440) (1.0 μg), pCMV-HA-Daxx-H4 (aa 110–500)(1.0 μg), pCMV-HA-Daxx-H5 (aa 500–740) (1.0 μg) were co-transfected with pFLAG-LANA (1.0 μg) (*left two panels*). PcDNA-Daxx-D1 (full-length) (1.0 μg), pcDNA-Daxx-D2 (deleted aa 271–509) (3.0 μg), pcDNA-Daxx-D3 (aa 63–740)(3.0 μg), pcDNA-Daxx-D4 (aa 111–740)(3.0 μg), and pcDNA-Daxx-D5 (aa 243–740) (2.0 μg) were individually co-transfected with pFLAG-LANA (1.0 μg) (*right two panels*). Immunoprecipitates (*IP*) with anti-FLAG antibody (M2) were followed by Western blotting (*WB*) with anti-HA antibody (*left panels*) or anti-Daxx antibody (*right panels*).

were produced in *E. coli*, and applied to pull-down assay with full-length ^{35}S-labeled LANA. The GST-fused full-length Daxx (G1) and the Daxx-deleted aa 500–740 (G2) bound to LANA, but deleted aa 440–740 (G3) failed (Fig. 4*B*). From the *in vitro* result above, the region of aa 440–500 in Daxx was thought to be critical for the binding. However, GST-fused aa 440–625 of Daxx (G4) did not bind (Fig. 4*B*), nor did any other mutants, although weak binding was observed with GST-fused aa 1–270 of Daxx (G8)(Fig. 4*B*). We constructed a series of deletion mutants of N-terminal HA-tagged Daxx (H2–H5), and co-expressed them with pFLAG-LANA in 293T cells. Immunoprecipitation with anti-FLAG antibody followed by Western blotting with anti-HA antibody showed that all the mutants except H5 bound to LANA (Fig. 4*C*, *left two panels*). The acidic-rich region (aa 440–500) of Daxx was not critical to the binding with LANA in cells, not corresponding with the results *in vitro*. To examine contribution of N terminus of Daxx, a series of mutant Daxx expression vectors with N-terminal deletion (D3–D5) and a deletion mutant without central region aa 271–509 (D2), were constructed and transiently expressed in 293T cells. Experiments of immunoprecipitation with anti-FLAG antibody and Western blotting with anti-Daxx antibody (sc-7152, that recognizes the C terminus of Daxx) showed that D3 bound firmly with LANA, but D4 did very little (Fig. 4*C*, *right two panels*). The first paired amphipathic helix (PAH), aa 63–108 appeared to be of some importance for the binding, although HA-tagged Daxx without PAH1 (H4) bound LANA. These results indicated that a central region aa 63–440 within Daxx,

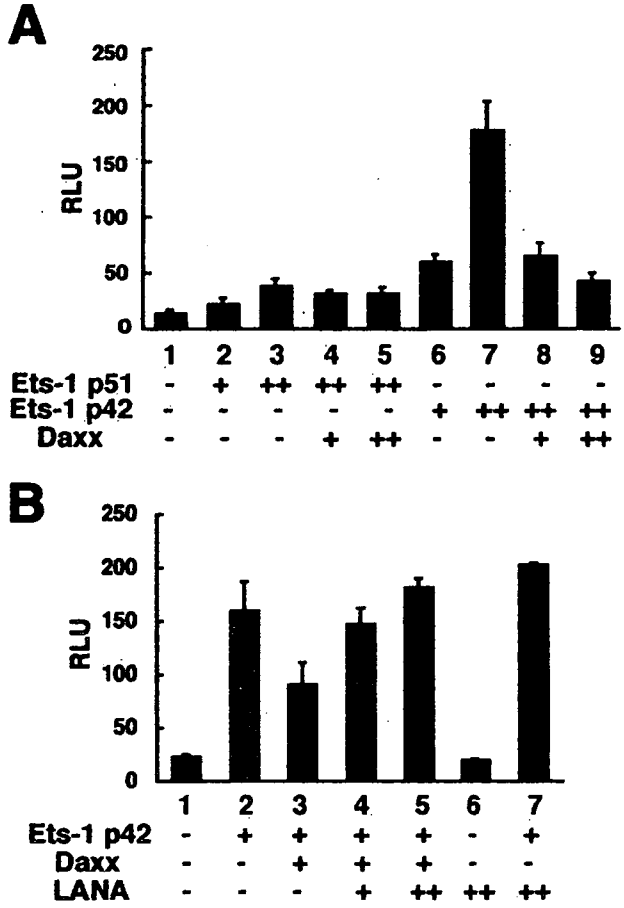

FIGURE 5. **LANA inhibited Daxx-mediated repression on Ets-1-dependent VEGF receptor 1 (Flt-1) gene expression.** *A*, Daxx repressed Ets-1-dependent Flt-1 expression. PcDNA-p51Ets-1 or pcDNA-p42Ets-1 (+; 25 ng, ++; 50 ng) were co-transfected with pcDNA-Daxx (+; 200 ng, ++; 500 ng) and pFlt-luc (100 ng). *B*, LANA counteracts Daxx-mediated repression in Flt-1 expression in the presence or absence of exogenous Daxx. PcDNA-p42Ets-1 (50 ng), pcDNA-Daxx (200 ng), and pFLAG-LANA (0, +; 50, ++; 100 ng, respectively) were co-transfected with pFlt-1-luc (100 ng). The relative luciferase activity (*RLU*) was normalized by β-galactosidase activity. Assays were performed in triplicate, and *error bars* indicate S.D.

containing two paired PAHs and its following 200 aa, was important for the binding with LANA in cells.

LANA Inhibited Daxx-mediated Repression of Ets-1-dependent VEGF Receptor 1 (Flt-1) Gene Expression— To examine the role of Daxx in Kaposi's sarcoma, we focused on Ets-1 transcription factor. It was reported that Daxx interacts with Ets-1 to repress Ets-1-dependent transcriptional activity of MMP-1 and Bcl-2 (12). On the other hand, as a characteristic feature of KS, it is known that VEGF and its receptors, Flt-1 and KDR (VEGF receptor-1 and -2, respectively), are highly expressed in KS (20). There are several Ets-1 motifs in Flt-1 and KDR promoters to regulate the expression (26) (27). We examined the effect of Daxx on Ets-1-dependent Flt-1 expression. We co-transfected a luciferase reporter plasmid pFlt-1-luc driven by Flt-1 promoter, an Ets-1 expression vector, and a Daxx expression vector into 293T cells, to perform luciferase assay. Transcriptional activity on Flt-1 increased depending on the amount of Ets-1 plasmid, although the effect of p51-Ets-1 was quite weak. Daxx evidently repressed Ets-1-dependent activation (Fig. 5*A*). p51 and p42 are two human variants of the Ets-1 molecule. It is reasonable that the activity of p51-Ets-1 is lower than p42-Ets-1 because p42-Ets-1 lacks exon VII, the internal transcriptional regulatory domain (24). This result is similar to the case of MMP-1 and Bcl-2 expression (28). As we observed the repressive activity of Daxx on Ets-1-dependent Flt-1 expression, we examined the effect of LANA on the Daxx-mediated repression with p42Ets-1. Co-transfection with a LANA expression plasmid dose-dependently reactivated the transcriptional activity repressed by exogenous Daxx (Fig. 5*B*, *4* and *5*), although LANA slightly activated it in the absence of exogenous Daxx (Fig. 5*B*, *7*). These results suggested that LANA inhibited the repression via interaction with Daxx.

LANA Activated Expression of VEGF Receptors in Vascular Endothelial Cells—To investigate the possibility that LANA induces Flt-1 in Kaposi's sarcoma lesion, we tried to express LANA in HUVEC, because endothelial cells (ECs) are regarded as the origins of KS lesions. We constructed a plasmid, pIRES2-LANA-GFP, which contains an internal ribosomal entry site (IRES) to express both LANA and GFP from a single mRNA. We transfected pIRES2-LANA-GFP or pIRES2-GFP as control into HUVEC and Flt-1 and KDR expression in GFP-positive cells were analyzed by flow cytometry. Flt-1 of GFP-positive cells in pIRES2-LANA-GFP-transfected cells was significantly increased as compared with that in control cells (Fig. 6*A*, *left*). The number of cells expressing Flt-1 over log intensity 1 (M1) was about 1.9× higher (Fig. 6*A*, *upper, right graph*) than that of control. M1 of KDR also increased 1.4× (Fig. 6*A*, *lower, right graph*). Furthermore, to examine the level of mRNA of the two receptors, we performed real-time PCR with total RNA prepared from the GFP-expressing HUVEC. LANA expression in pIRES2-LANA-GFP-transfected cells was confirmed by using PCR with primers of LANA (data not shown). The relative expressions of Flt-1 and KDR in LANA-expressing cells were 1.4 and 2.0× higher than that of control cells, respectively (Fig. 6*B*). Although there was discrepancy between rise of protein and mRNA, results of both FACS and real-time PCR indicated that LANA induced the two receptors in human endothelial cells. The expression of Ets-1 and Daxx was not altered between LANA-expressing cells and control cells (Fig. 6*B*).

LANA Sequesters Daxx from Ets-1—To resolve the mechanism of the activation of VEGF receptors expression by LANA, we examined the relation of the three molecules, LANA, Daxx, and Ets-1. 293T cells were co-transfected with a constant amount of pcDNA-Daxx and pcDNA-Ets-1, and a variable amount of pFLAG-LANA. Nuclear extracts were prepared and subjected to immunoprecipitation and Western blotting with anti-Ets-1 antibody, anti-Daxx antibody or anti-FLAG antibody. Daxx and Ets-1 were expressed in a fixed amount (Fig. 7*A*, *row a*), *middle and right panel*, respectively) and FLAG-LANA was dose-dependently increased in the nuclear extract (Fig. 7*A*, *row a, left panel*). When we performed immunoprecipitation with anti-FLAG antibody, Daxx was detected in the immune complex in proportion to the amount of LANA (Fig. 7*A*, *row b, middle panel*). On the other hand, we detected no specific interaction between LANA and Ets-1 in the immune complex (Fig. 7*A*, *row b, right panel*). Next, by immunoprecipitation with anti-Daxx antibody, FLAG-LANA was detected in direct proportion to the amount of LANA (Fig. 7*A*, *row c, left panel*). The immune complex also contained Ets-1 in inverse

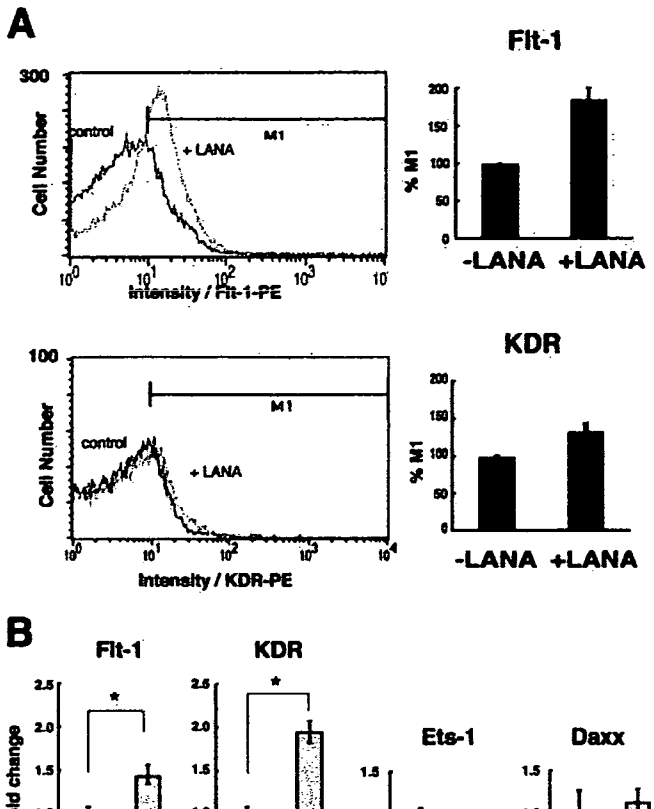

FIGURE 6. **LANA induced VEGF receptors in HUVEC.** *A*, flow cytometric analysis of Flt-1 (*upper graphs*) and KDR (*lower graphs*) expression of control (pIRES2-GFP transfected cells; *black lines*) and LANA-expressing cells (pIRES2-LANA-GFP-transfected cells; *gray lines*). The graphs to the *right* of each indicate percentages of cells that exceed 1 of the relative log intensity (*M1*). Experiments were repeated three times and the M1 values represent means of the three experiments; *error bars* indicate S.D. *B*, real-time PCR analysis of Flt-1, KDR, Ets-1, and Daxx. HUVECs transfected transiently with pIRES2-LANA-GFP or pIRES2-GFP (as a control) were sorted 2 days after transfection. Total RNA extracted from the cells (1 μg) was reverse-transcribed to cDNA (40 μl), and aliquots (0.4 μl) were applied to real-time PCR (20 μl) with each primer (0.4 mM) in triplicate described under "Experimental Procedures." Values represented relative expression of Flt-1, KDR, Ets-1, and Daxx (calculated with threshold cycle number, CT) of LANA-expressing cells compared with that of control cells. Each value was adjusted with CT of internal control (GAPDH). *, p value < 0.02.

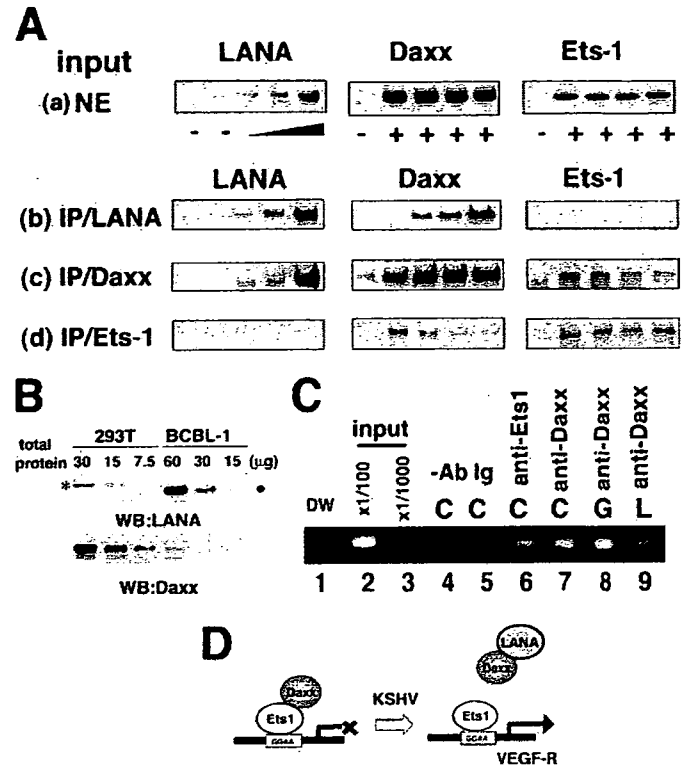

FIGURE 7. **LANA interacted with Daxx to sequester from Ets-1.** *A*, Western blotting analysis of immunoprecipitates with anti-FLAG, anti-Daxx, and anti-Ets-1 antibodies. 293T cells were transfected with a constant amount of pcDNA-Daxx (2 μg) and pcDNA-p42Ets-1 (2 μg), and an increasing amount of pFLAG-LANA (0.25, 0.5, 1.0 μg). Total DNA amounts were adjusted with pFLAG-CMV-2 vector to be 5 μg. Nuclear extracts (*row a*), immune complex using anti-FLAG antibody (*row b*), immune complex using anti-Daxx antibody (*row c*), and immune complex using anti-Ets-1 antibody (*row d*), were subject to Western blotting with anti-FLAG antibody (*left*), anti-Daxx antibody (*middle*) or anti-Ets-1 antibody (*right*). *B*, relative protein amounts of LANA and Daxx in BCBL-1 cells and those of transfected 293T cells. 293T cells were co-transfected with pcDNA-Daxx (2 μg), pcDNA-p42Ets-1 (2 μg), and pFLAG-LANA (1.0 μg). Nuclear extract (30, 15, 7.5 μg of the 293T cells and 60, 30, 15 μg of BCBL-1 cells) were subjected to Western blotting with anti-LANA antibody or anti-Daxx antibody. FLAG-LANA (*) migrated slower than native LANA(●) did. *C*, chromatin immunoprecipitation of Ets-1 and Daxx interaction with Flt-1 promoter in HUVECs. Bands indicate PCR products targeting −90 to +8 of Flt-1 promoter. 2 μl of water (*lane 1*), 1/100 and 1/1000 of input (cross-linked and sonicated pre-immunoprecipitation lysate) (*lanes 2* and *3*), eluate from no antibody (*lane 4*), rabbit IgG (2 μg) (*lane 5*), anti-Ets-1 antibody (2 μg) (*lane 6*), and anti-Daxx antibody (2 μg) (*lane 7*) were applied to the PCR reaction, respectively. Eluate from anti-Daxx antibody of LANA-expressing HUVECs (*L*, *lane 9*) and that from the control GFP-expressing HUVECs (*G*, *lane 8*) were subjected to PCR reaction. *D*, possible mechanism for induction of VEGF receptors by LANA. Daxx interacts with Ets-1, and represses Ets-1-dependent expression in the absence of LANA, while LANA sequesters Daxx from Ets-1 to inhibit the interaction between Daxx and Ets-1, resulting in activation of Ets-1-dependent expression of VEGF receptors.

proportion to LANA expression (Fig. 7*A*, *row c*, *right panel*). Consistently, Daxx was detected in the immune complex with anti-Ets-1 antibody in inverse proportion to LANA expression (Fig. 7*A*, *row d*, *middle panel*). LANA was not detected in the immune complex with the anti-Ets-1 antibody (Fig. 7*A*, *row d*, *left panel*), which implies that increasing LANA caused increase of Daxx-LANA interaction, and reduction of Daxx-Ets-1 interaction. These results suggested that LANA sequesters Daxx from Ets-1, which results in inhibition of the interaction between Daxx and Ets-1.

In the experiments above we used transiently transfected 293T cells (Fig. 7*A*). To address whether the transient expression system for LANA-Daxx interaction is physiologically relevant or not, we analyzed relative expression levels of LANA and Daxx proteins using BCBL-1 and the transfected 293T cells. As shown in Fig. 7*B*, the expression level of exogenous LANA protein in 293T cells in the same condition of Fig. 7*A* was similar to that of endogenous LANA in BCBL-1 cells. In contrast, endogenous Daxx expression level is much lower in BCBL-1 cells than in the 293T cells. These data indicated that relative expression ratio of endogenous LANA to Daxx in BCBL-1 cells was much higher than that of LANA-transfected 293T cells.

Daxx associated with Flt-1 promoter and LANA reduced its association in HUVEC. To investigate the possibility that Daxx affects transcriptional activity of Ets-1 for Flt-1 expression in endothelial cells (ECs), we performed ChIP assay using HUVEC. Cross-linked nuclear extract from HUVECs was immunoprecipitated with anti-Ets-1 antibody or anti-Daxx